Scanning and Analytical Transmission Electron Microscopy

Introduction to STEM

MSE-735

Fall 2025

Emad Oveisi

Contents

Types of transmission electron microscopes

Emad Oveisi

Conventional mode (CTEM)

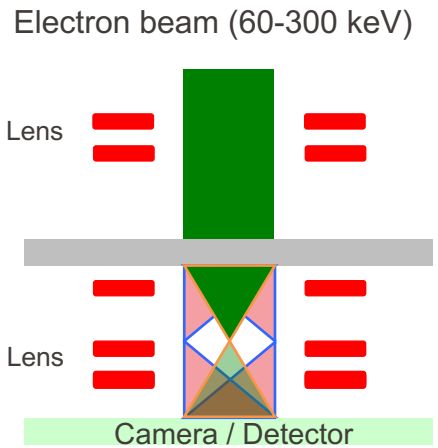

The most important lens:
Objective lens

Sample

Scanning mode (STEM)

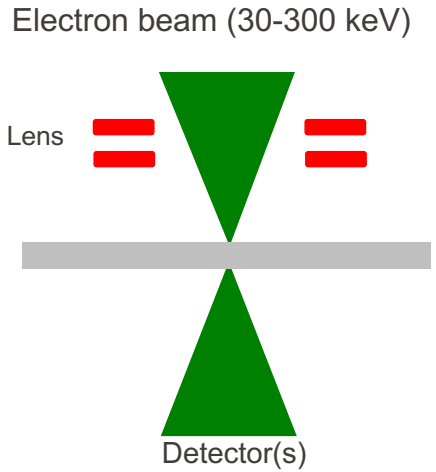

The most important lens:
Condenser lens

Emad Oveisi

Principles of STEM

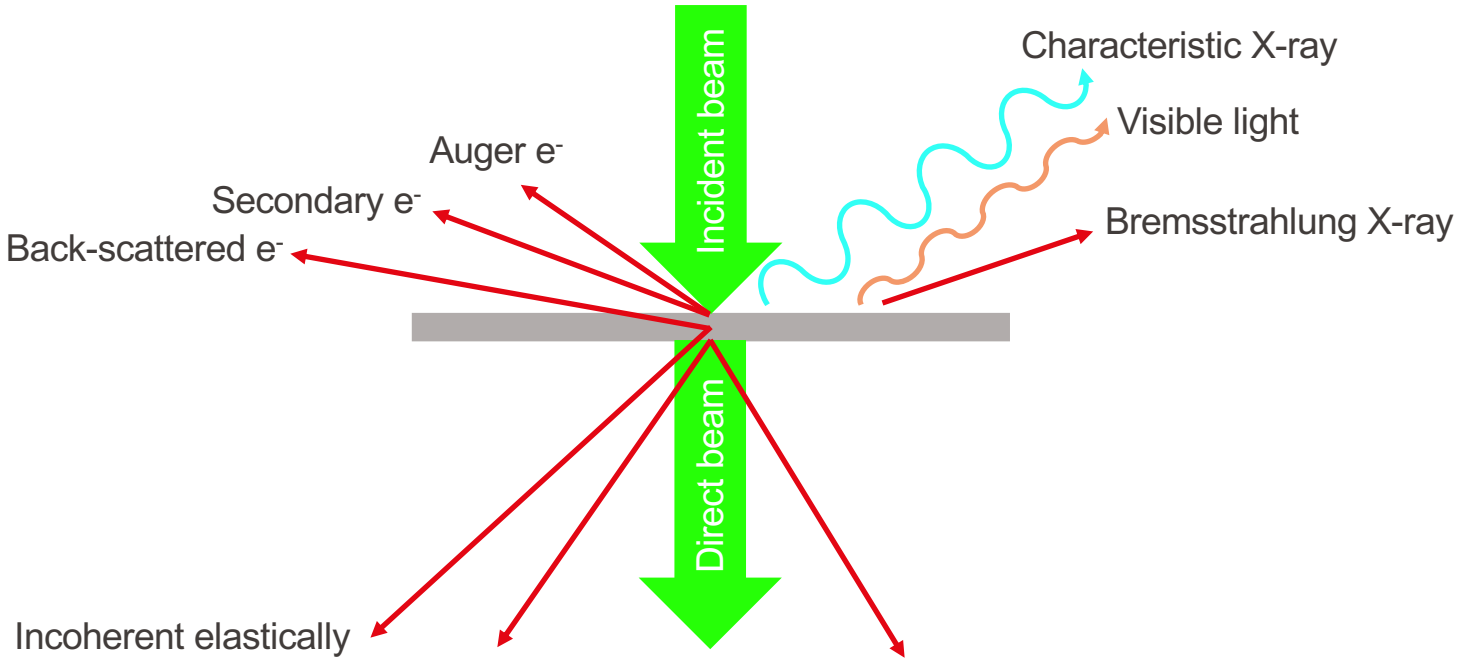

Emad Oveisi

Principles of STEM

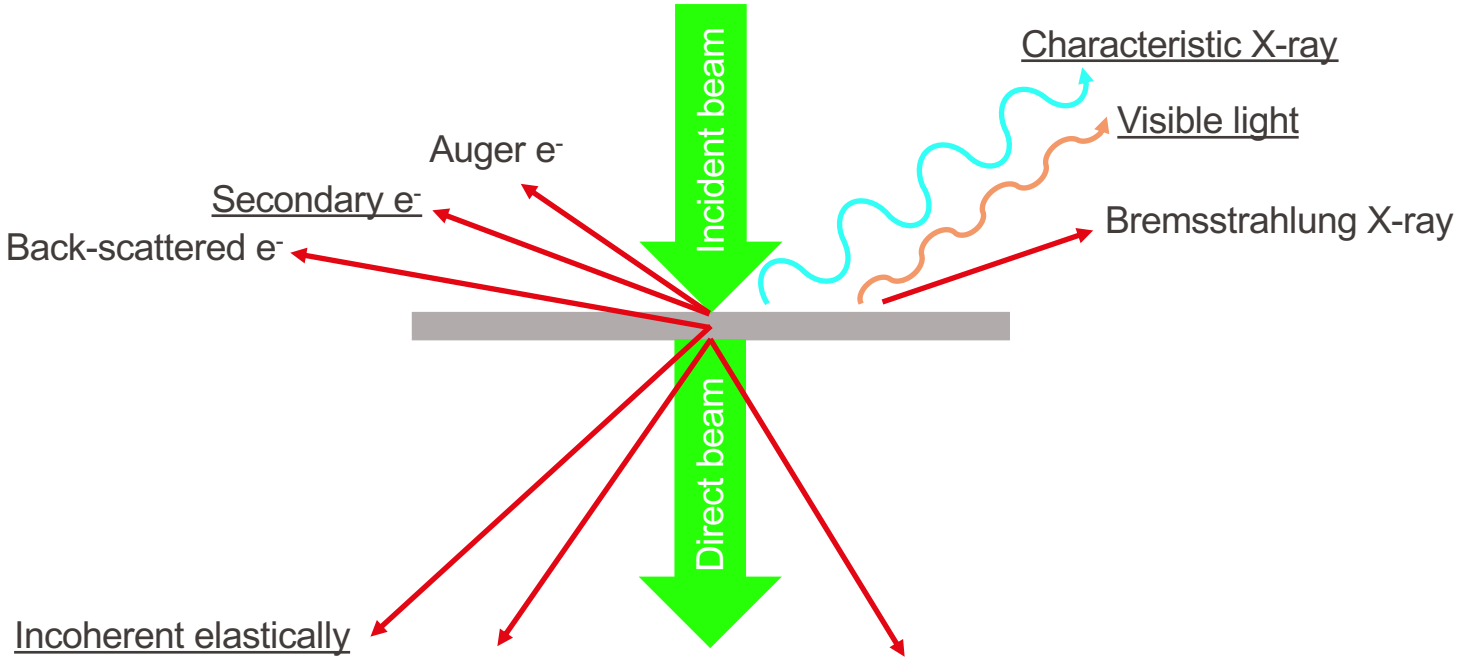

Principles of STEM

In STEM, the electron beam is focused to a fine spot (sub-Ångström in size for aberration-corrected STEMs), which is then scanned over the sample in a raster pattern. This is similar to the operation of scanning electron microscopy.

By rastering the beam across the sample, STEM is well suited for analytical spectrum imaging techniques such as EDX and EELS.

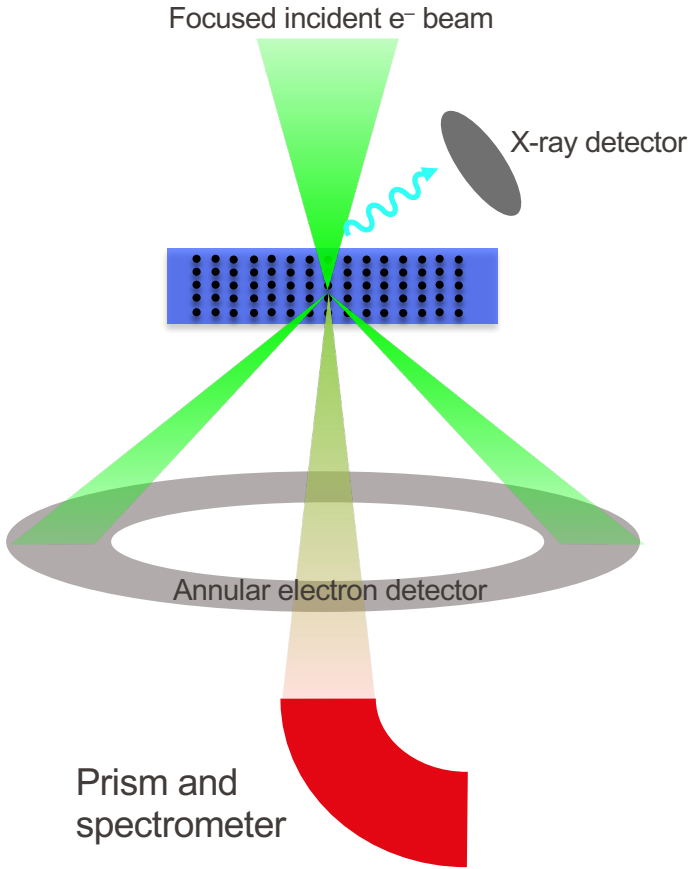

Principles of STEM

Electromagnetic lens (condenser system): Focuses electrons from the FEG onto the sample.

Beam deflectors: Scan the beam across the sample.

For each probe position (x, y):

- Detector:
Records signal intensity I(x,y) → forms an image.

- Spectrometer:
Records integrated signals from hyperspectral datasets
→ forms a 3D data cube (e.g., EELS or EDX spectrum image).

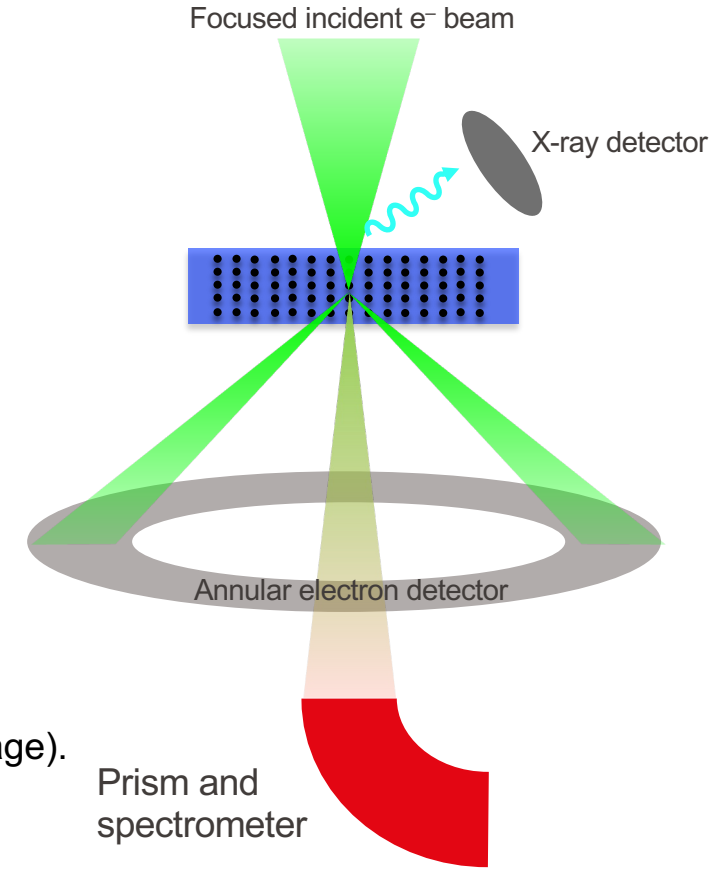

Principles of STEM | Magnification and scanning

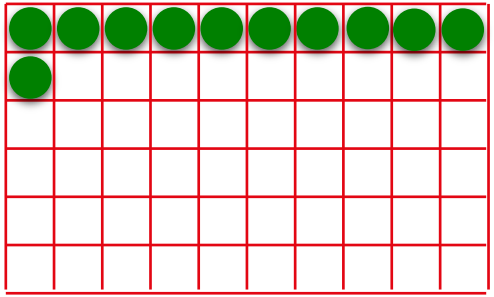

Beam locations on the specimen

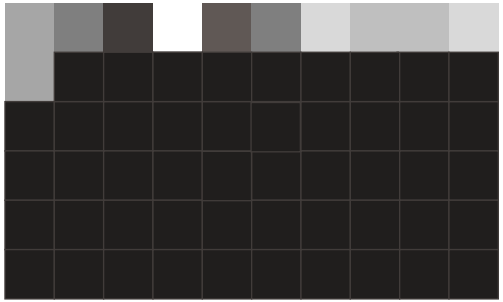

Area scanned on the screen

Information transfer f(x,y,S)

- Image formed by recording the time sequence of intensities for any particular small portion of diffraction pattern as the incident beam is scanned over the sample (using pair of deflector or scan coils)
- Monitor and scanning coils are synchronized
- Intensity of each pixel is proportional to signal collected by the detector
- When changing the magnification, we just change the raster size (no change in optics)

Magnification = Image size (e.g. display) / Raster size on the specimen

Principles of STEM | Magnification and scanning

All the STEM images appear on the computer screen at a magnification that is controlled by the **scan dimensions** on the specimen, not the lenses of the microscope.

This is a fundamental difference between scanning and static image formation.

Magnification = Size of the screen / Raster size on the sample

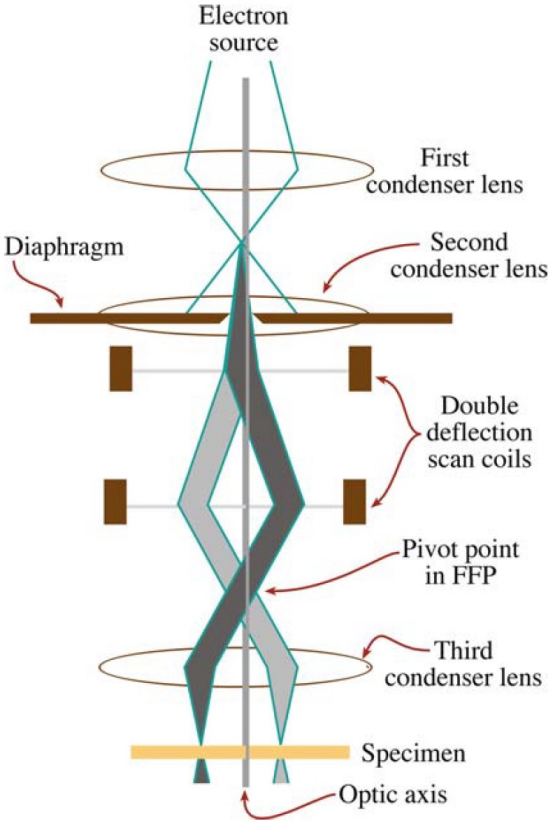

Principles of STEM | Magnification and scanning

Emad Oveisi

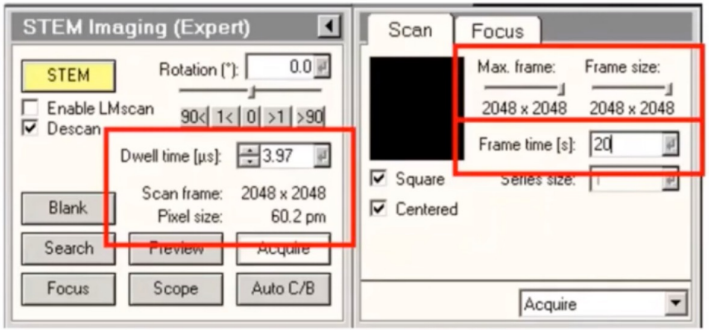

Scan frame × Dwell time = Frame time

Example: 2048×2048 pixels × 3.97 µs per pixel ≈ **20 s**

If for Mag. = 640 kx, the Pixel size is 60.2 pm, for Mag. = 2.55 Mx calculate:

a) The pixel size,
b) Scan area, and
c) Size of the screen

Emad Oveisi

Probe forming | 2-condensor lens system

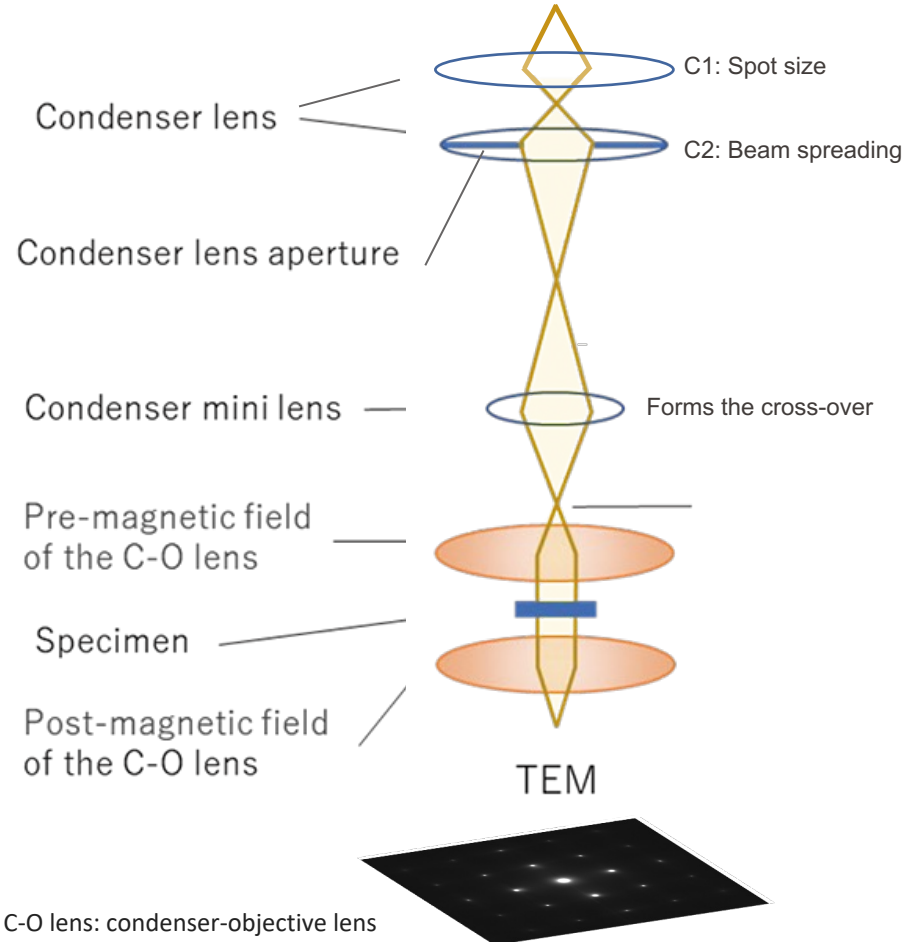

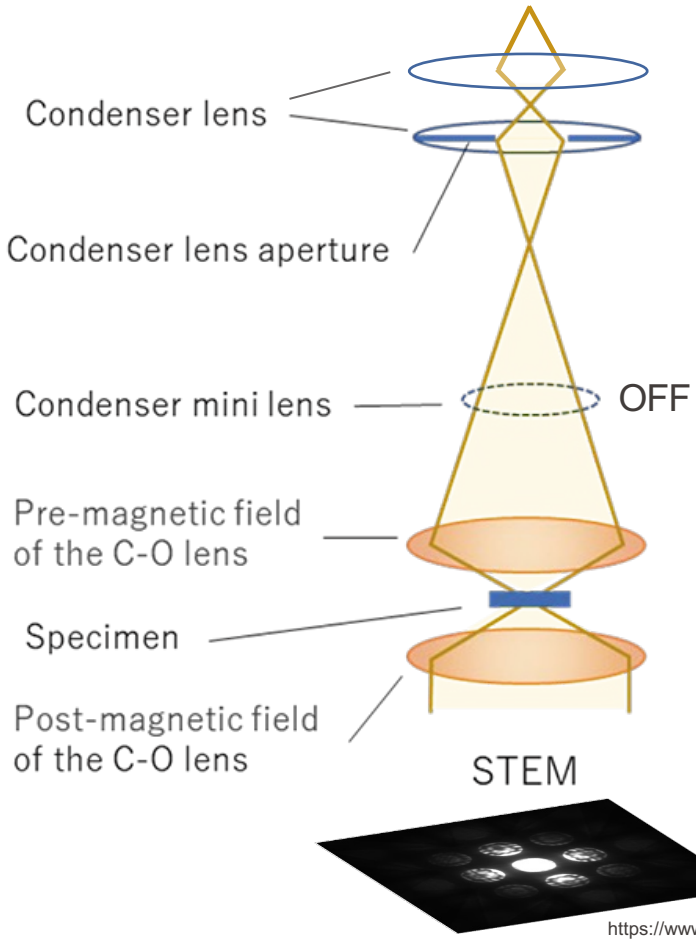

C-O lens: condenser-objective lens

https://www.jeol.com/

Probe forming

Consider exact 2-beam condition:

Imagine a convergent beam, not fully focused on sample
→ Decompose as parallel rays of different directions

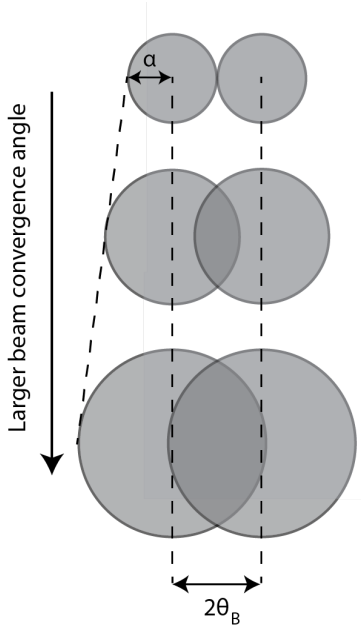

hkl disks

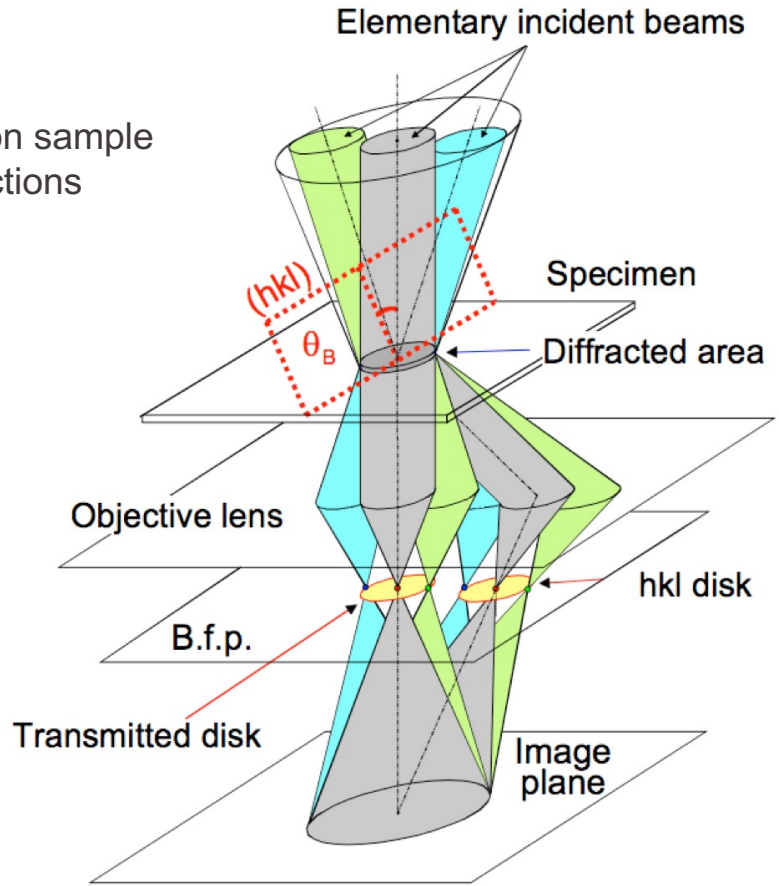

Figures by Jean-Paul Morniroli

Probe forming

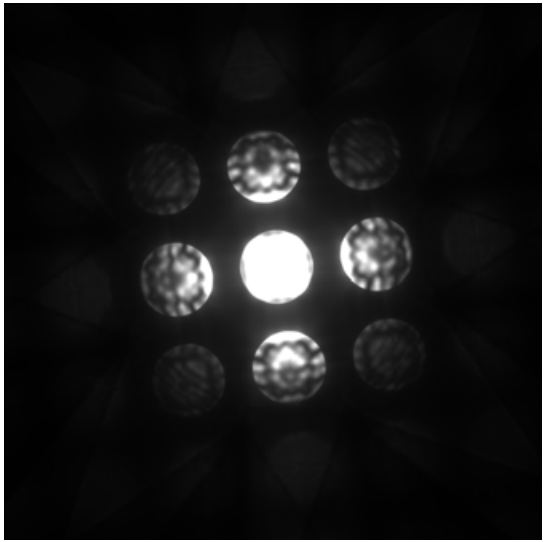

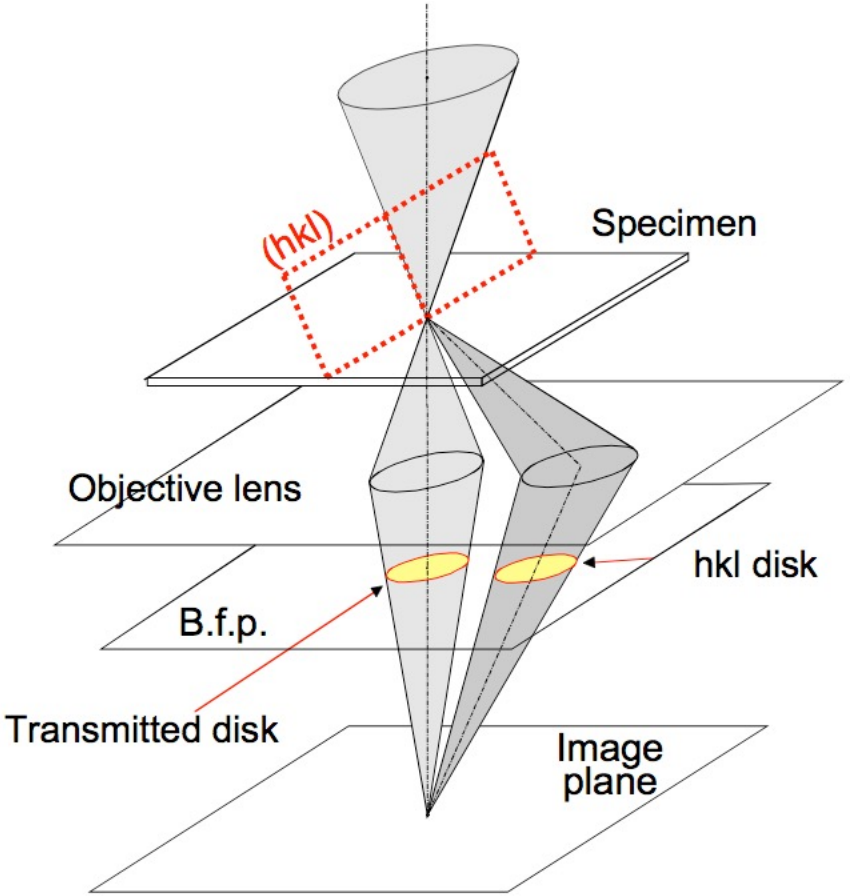

Probe forming | 3-condensor lens system

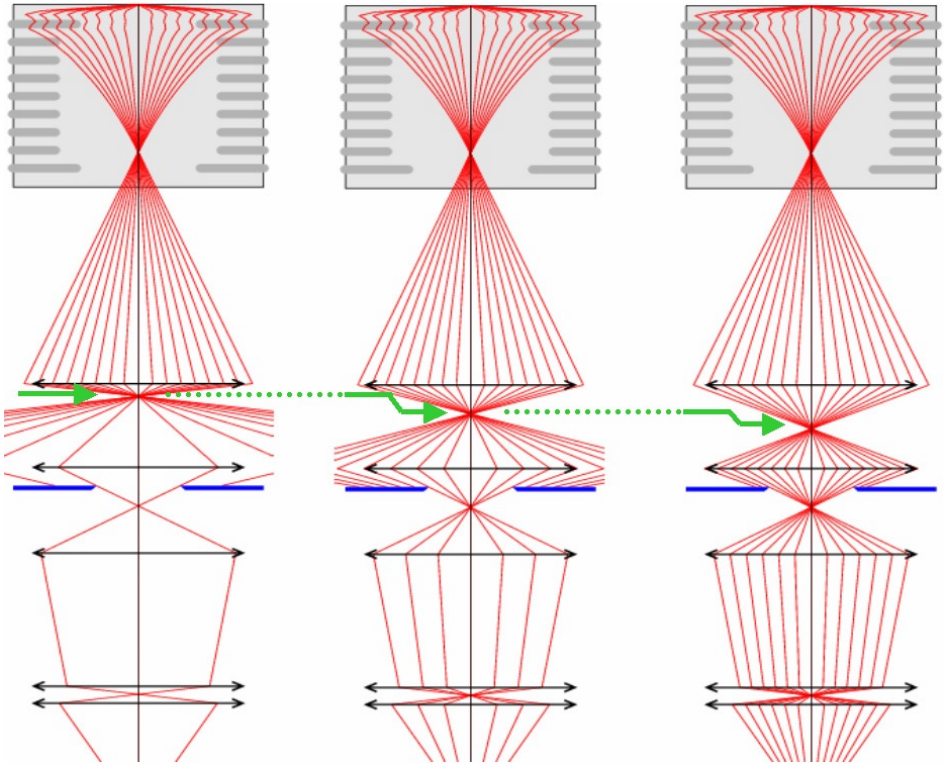

Emad Oveisi

Probe forming | 3-condensor lens system

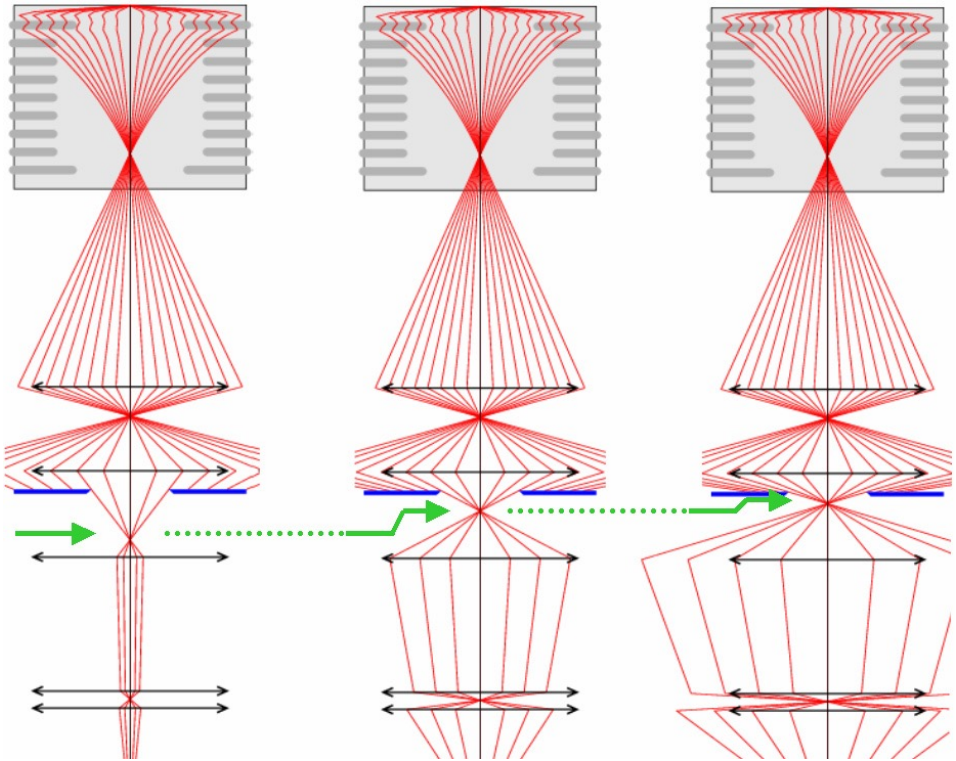

Aberrations

Ideal lens

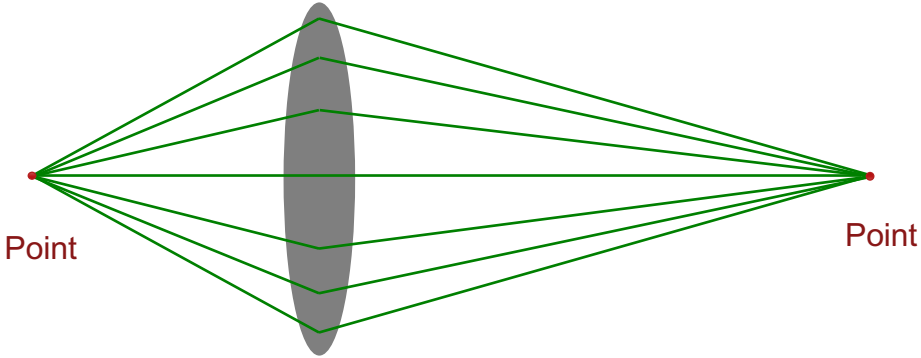

A point source is focused to a point

Real lens

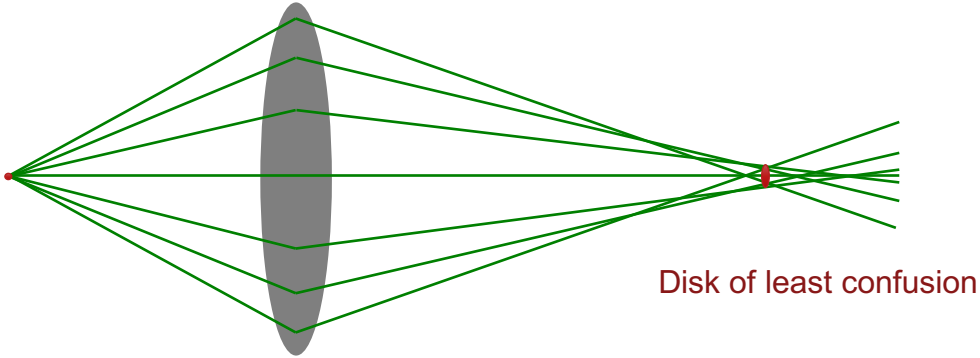

A point source is focused to a disk

Lens aberrations limit resolution!

Emad Oveisi

Aberrations

- **Lens aberrations**
  - Chromatic aberration
  - Spherical aberration
  - Astigmatism

Diffraction effect (aperture limit)

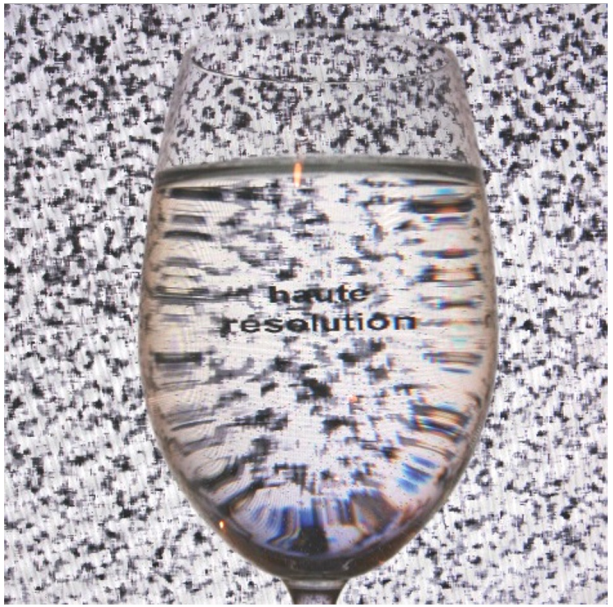

STEM resolution is detemined by the size of the probe and stability of the instrument

Resolution in HR-S/TEM limited by aberrations, especially by Spherical aberration (C_S)

Aberrations

- Spherical aberration (Cs)

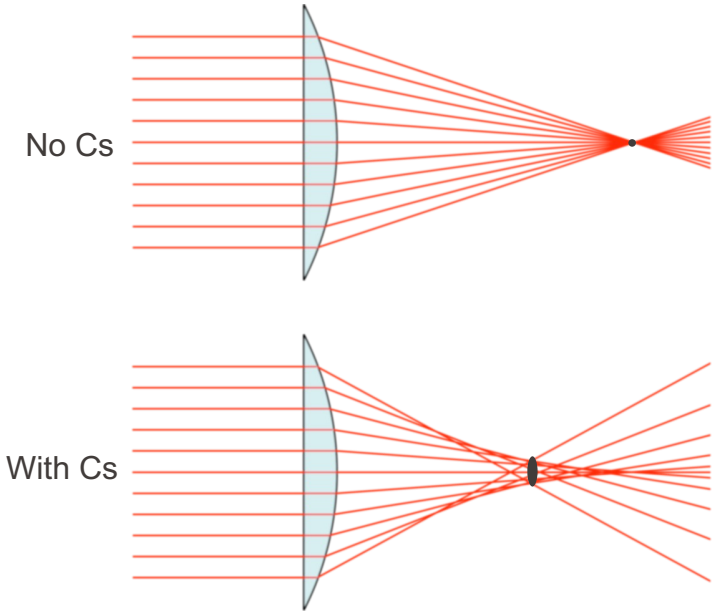

- Parallel rays that pass through the central region of the lens focus farther away than the rays that pass through the edges of the lens.
- Results in multiple focal points and thus a blurred image.
- Larger probe and lower resolution.

Core of the galaxy M100 ©NASA

Aberrations

- Spherical aberration (Cs)

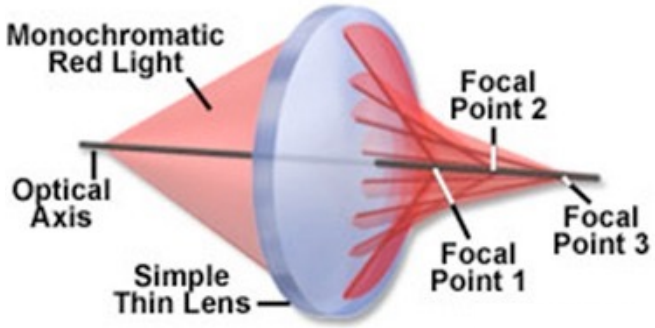

$$\alpha_{opt} = \left(\frac{4\lambda}{C_s}\right)^{\frac{1}{4}}$$

$$d_{opt} = 0.61\,\frac{\lambda}{\alpha_{opt}} = 0.43\,\lambda^{\frac{3}{4}}\,C_s{}^{\frac{1}{4}}$$

- Focal length depends on the distance from optical axis
- Image of the object is dispersed along the optical axis

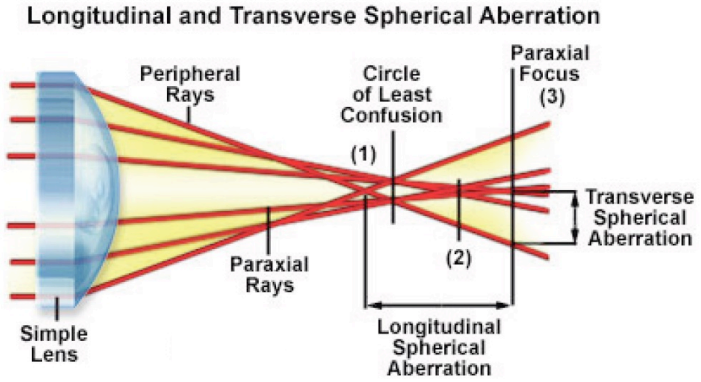

Aberrations

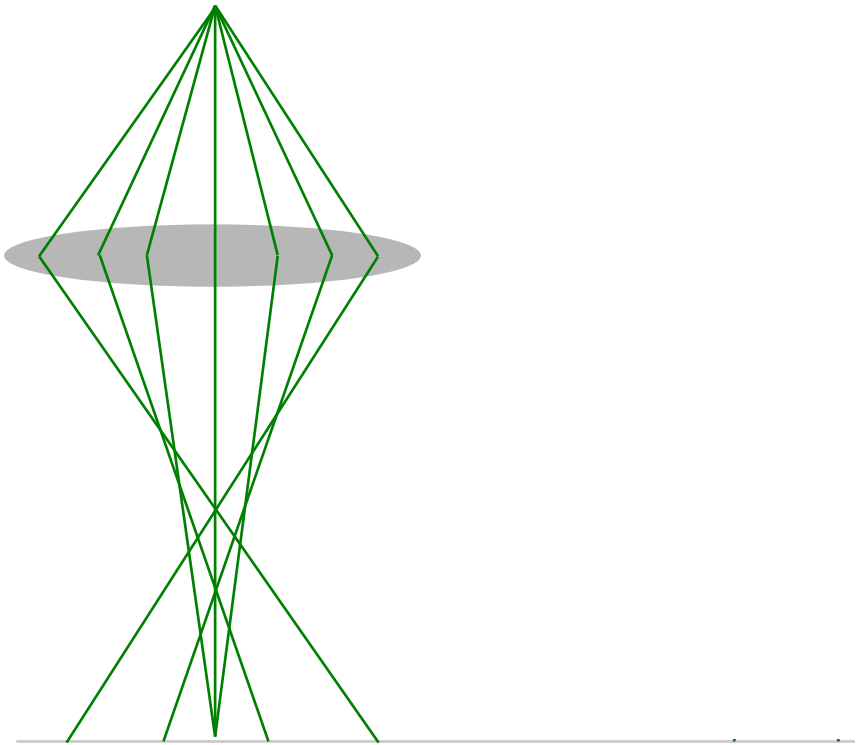

How to lower the effect of spherical aberration?

Aberrations

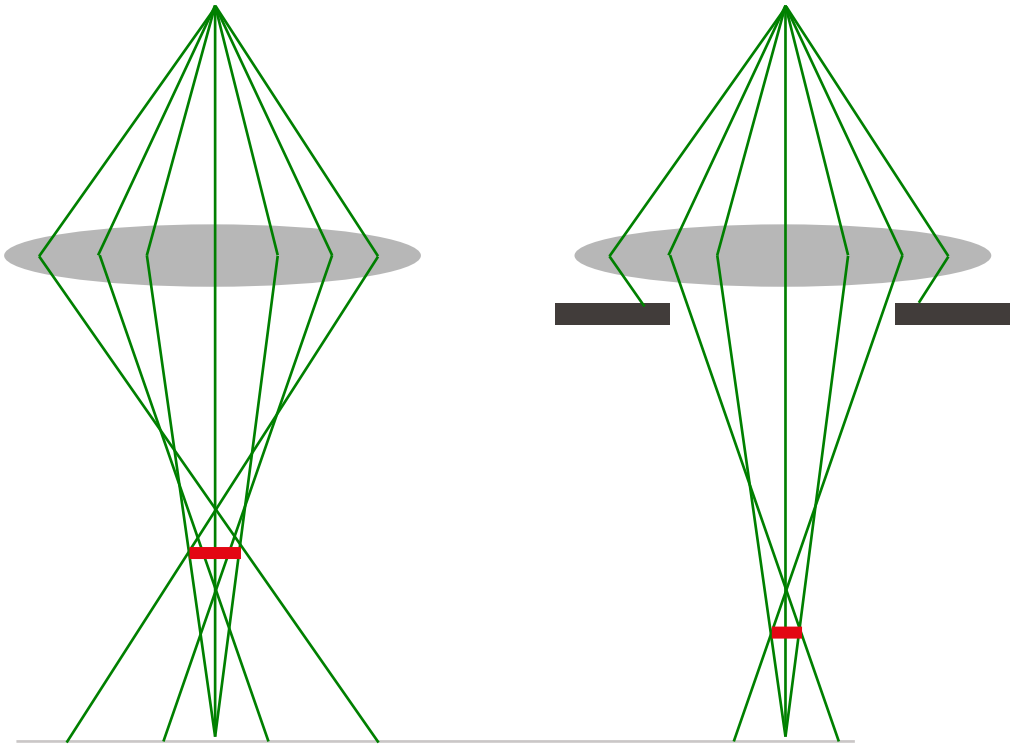

Inserting an aperture can lessen the effect of spherical aberration

But it comes with a cost → Lower current and more diffraction effect

Emad Oveisi

Aberrations | Correctors

- Cs correction in light optics
  - Correction with combination of convex and concave lenses

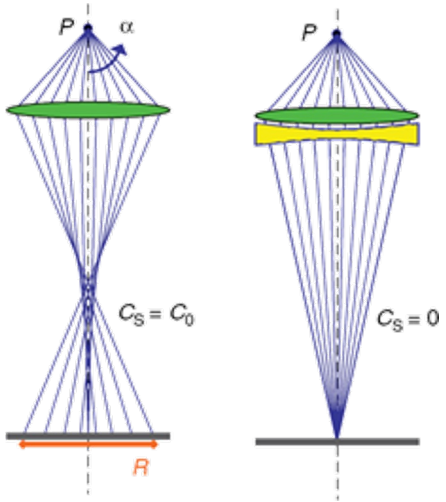

- Cs correction in electron optics
  - Combination of standard radially-symmetric convergent lenses with multipole divergent lenses (e.g. tetrapoles, hextapoles) to tune C_S.
  - Compensate Cs and other distortions with equivalnt but opposite componenets to add together with aim of giving ideal spherical wavefront

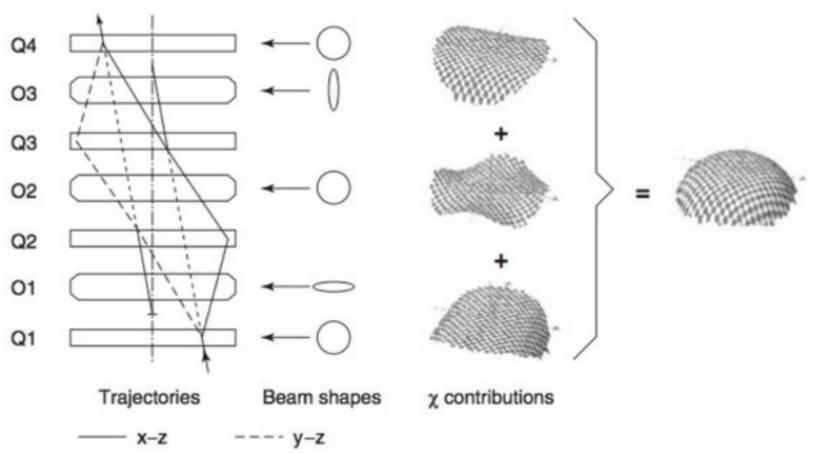

Krivanek et al. Aberration Correction in Electron Microscopy, Handbook of Charged Particle Physics 2009, pp. 601–641
http://www.sfc.fr/Material/hrst.mit.edu/hrs/materials/public/ElecMicr.htm

Aberrations | Resolution

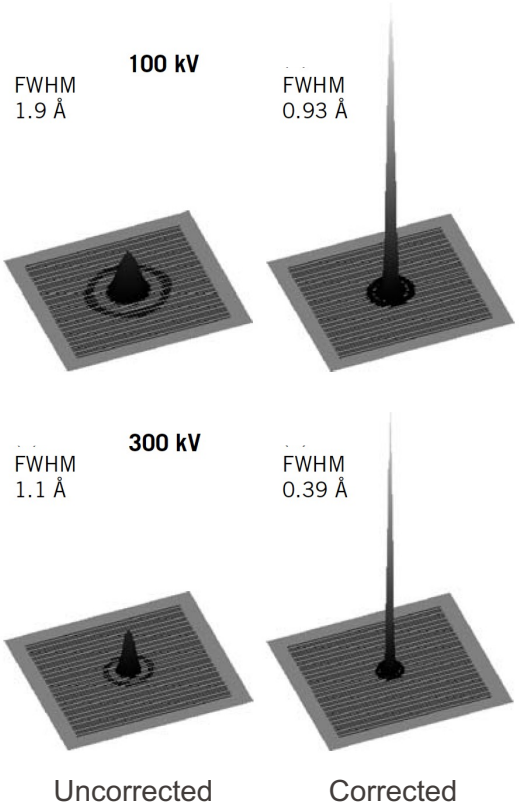

Z-contrast images

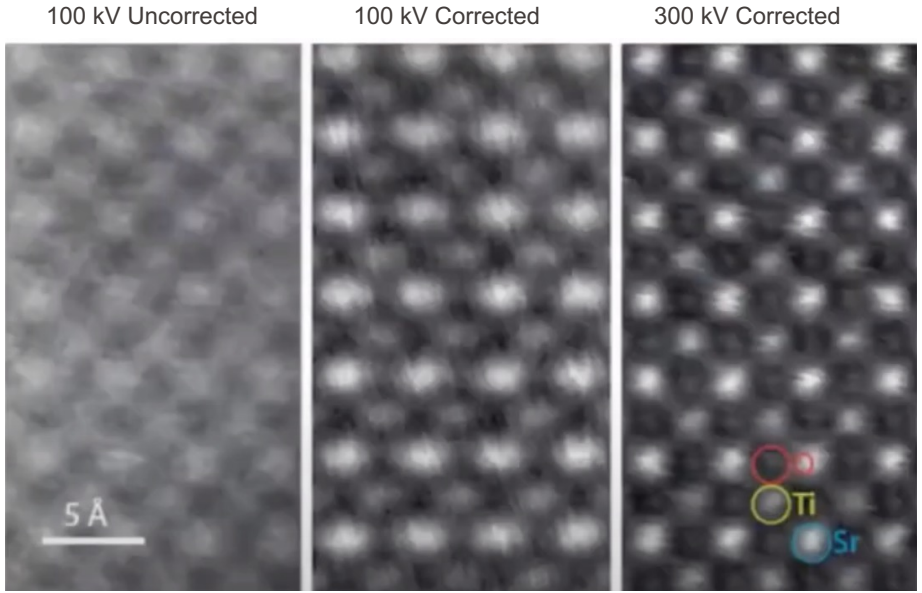

Advances in Imaging and Electron Physics 153, Peter W. Hawkes (Eds.)

Aberrations

- Chromatic aberration (Cc)

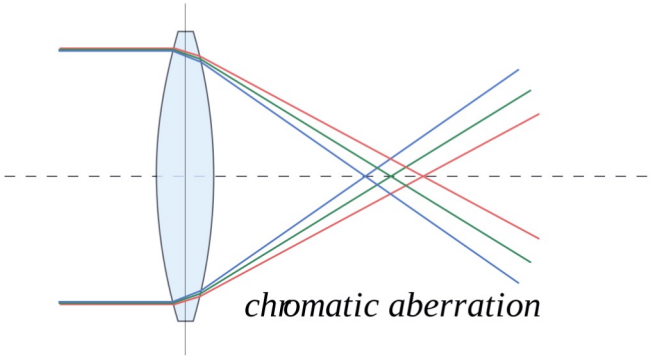

- Lens cannot focus all energies to the same convergence point.
- Electrons of lower energy will be bent more strongly.
- Correcting the aberration is necessary, otherwise the resulting image would be blurry and delocalized, a form of aberration where periodic structures appear to extend beyond their physical boundaries.
- The effect of Cc increases with source energy spread.

Image formation

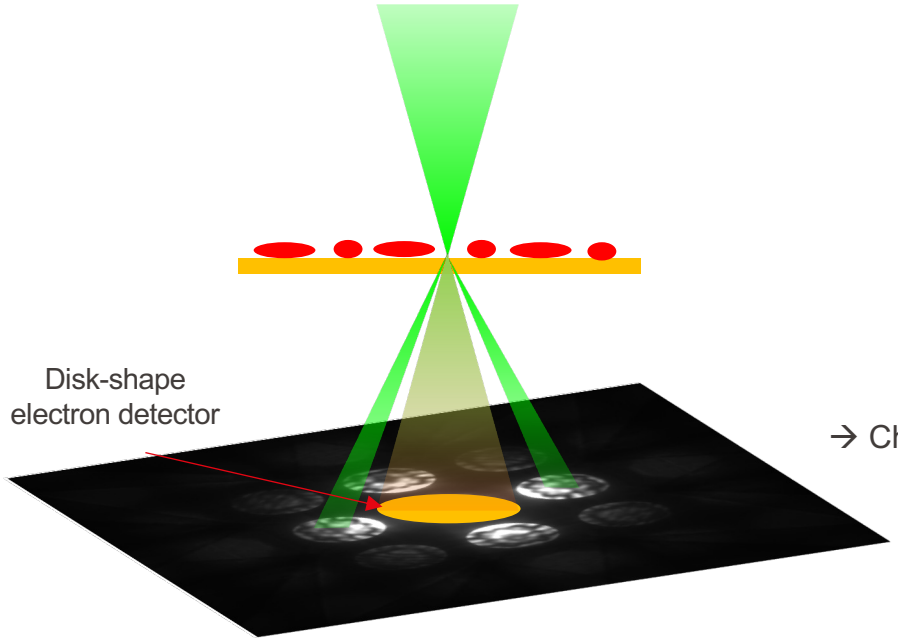

Scan position (x,y)

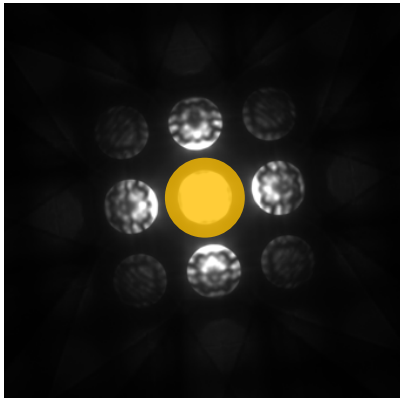

Defects, crystal tilts relative to incident or chenges in thickness,
→ Change in diffraction condition and intensities

→ Change in integrated signal on detector → Signal change on the image

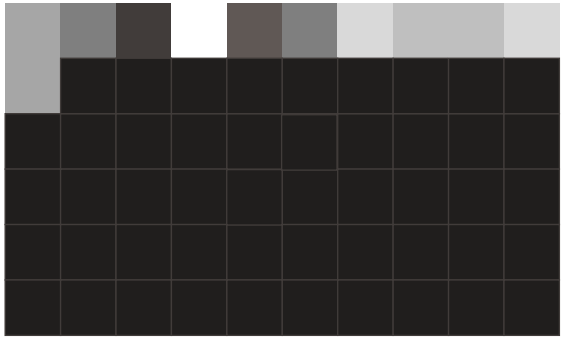

Image formation

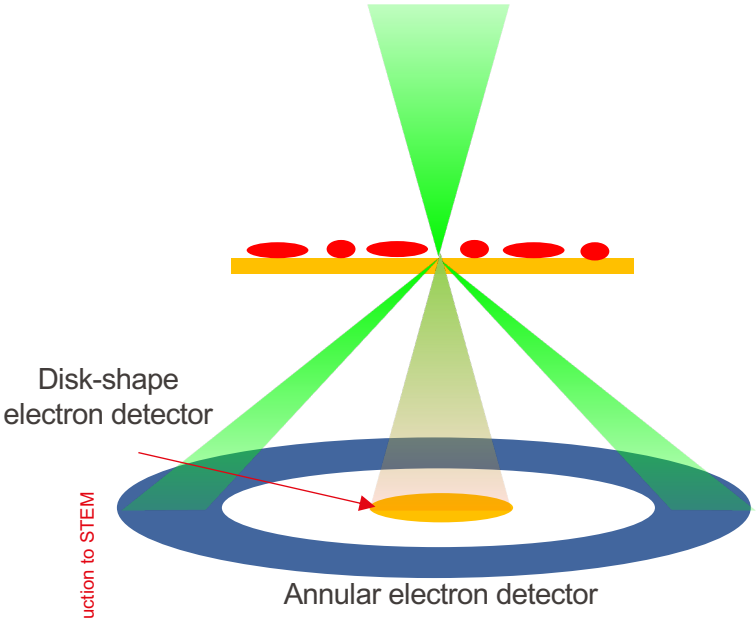

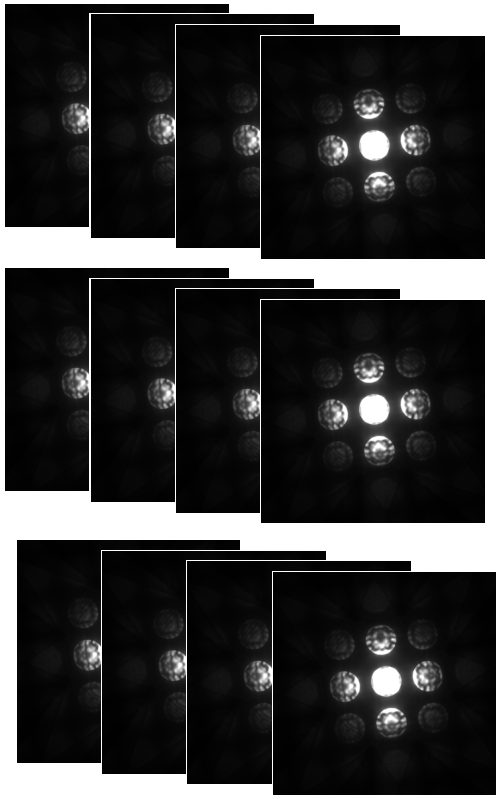

BF: Bright-field
ADF: Annular dark-field

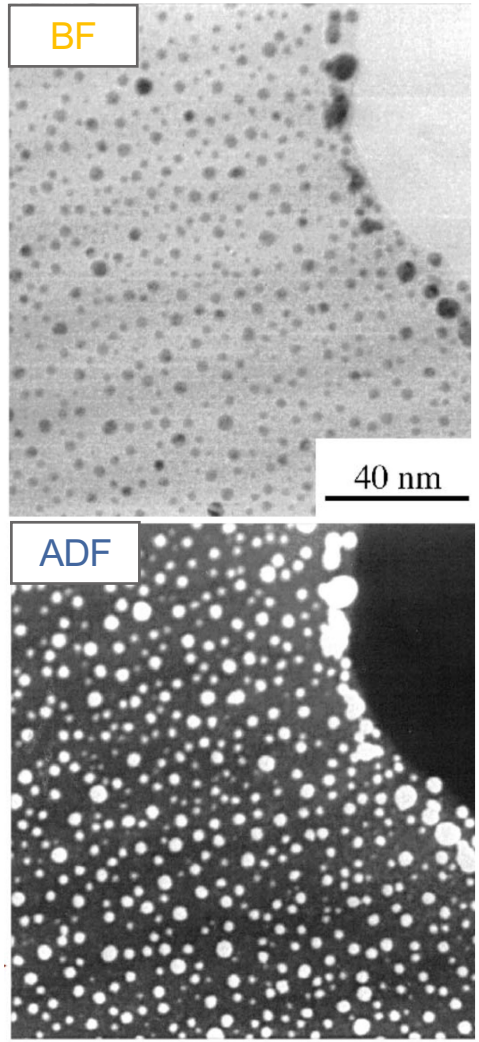

Principles of STEM | Knowledge of angles

Emad Oveisi

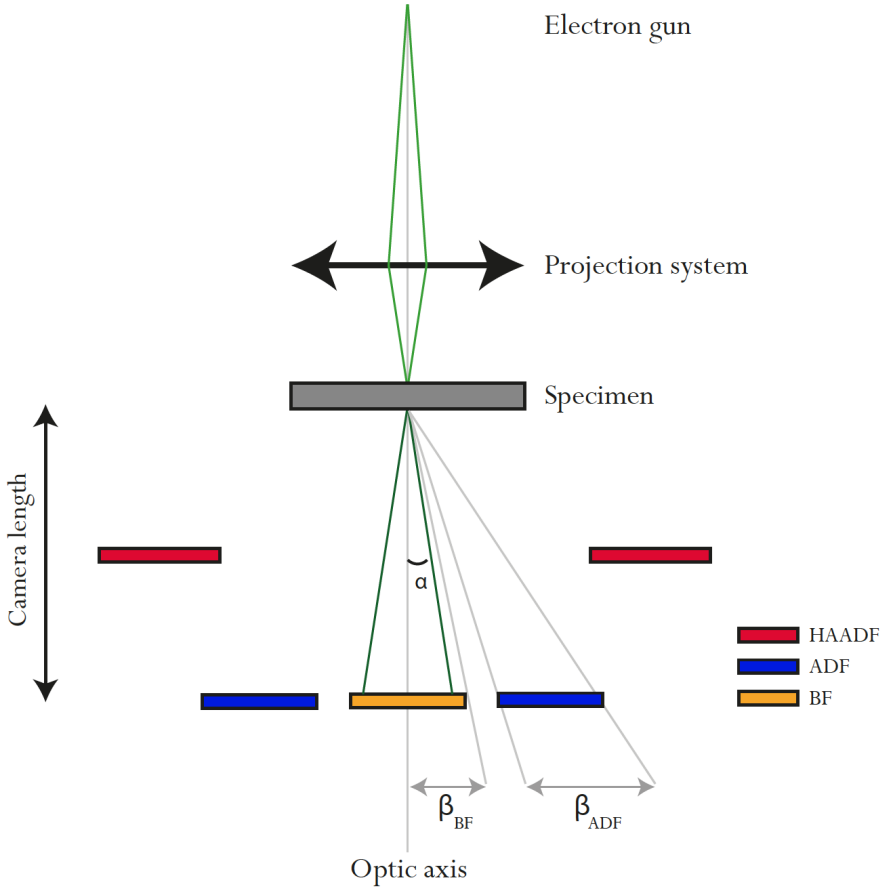

The focused probe is a convergent electron beam.

The BF and ADF detectors are radially symmetric. Therefore, they are characterised by the range of scattering angles they collect.

The convergence semi-angle of the probe is denoted by **α**.

A collection semi-angle of a detector is denoted by **β**, which may be defined by an inner and outer collection angle:

β_{inner} : the minimum scattering angle collected
β_{outer} : the maximum scattering angle collected

Knowledge of these angles is important for STEM imaging.

Principles of STEM | Knowledge of angles

Emad Oveisi

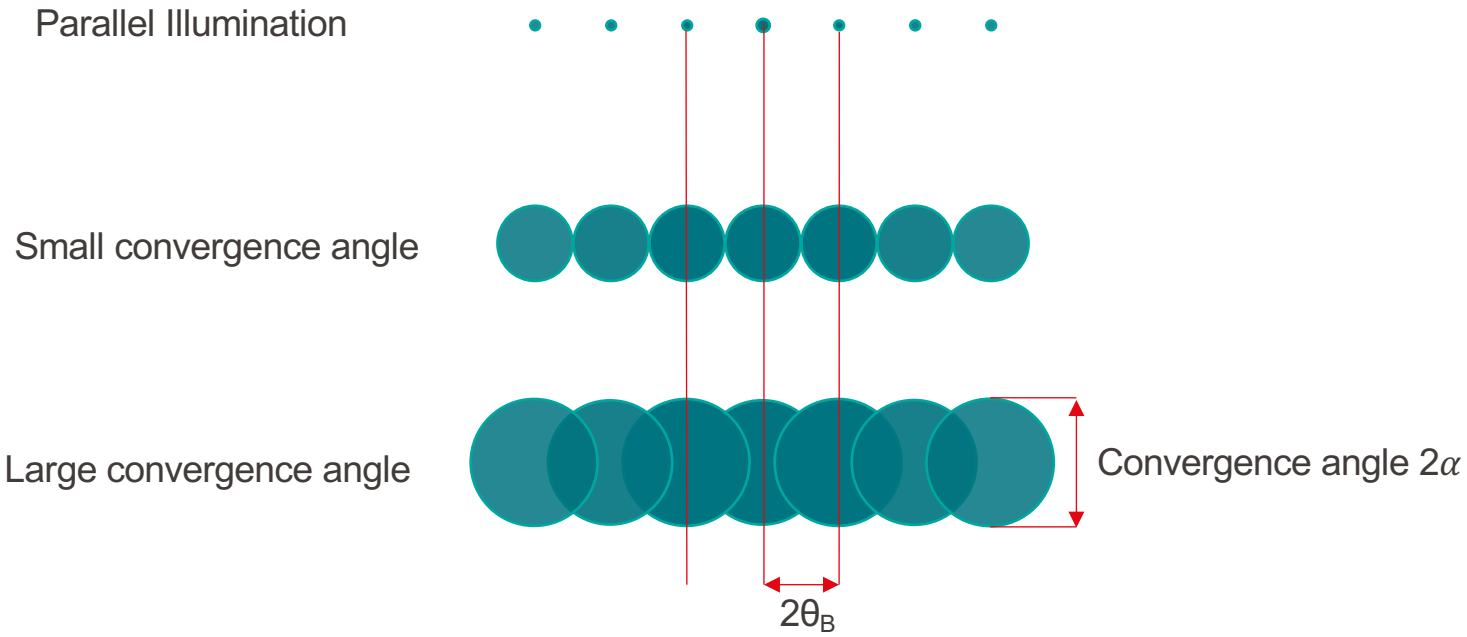

Disks overlap if $\theta_B < \alpha$

Principles of STEM | Knowledge of angles

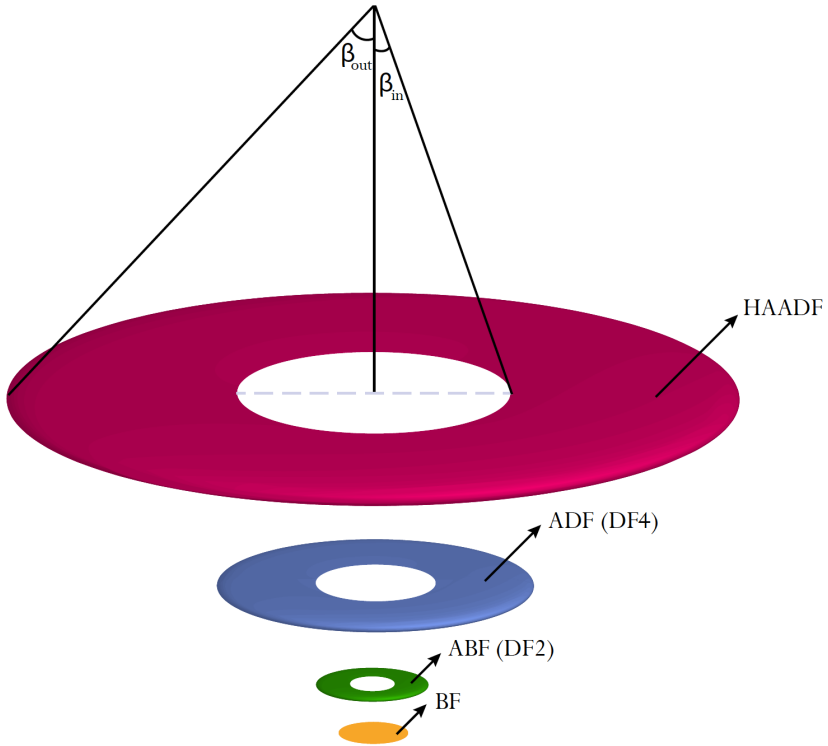

Schematic showing the configuration of the STEM detectors in the Osiris, Themis, and Spectra installed at CIME.

Principles of STEM | Knowledge of angles

Emad Oveisi

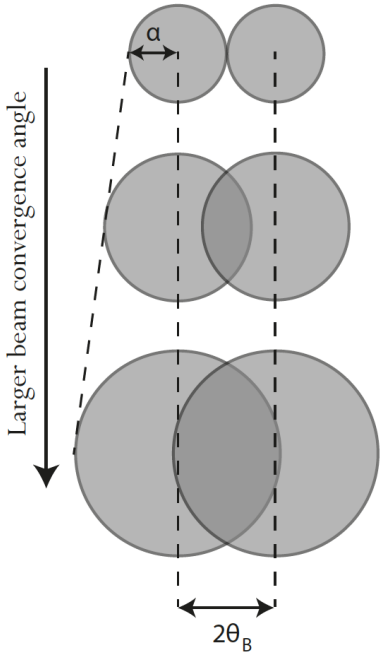

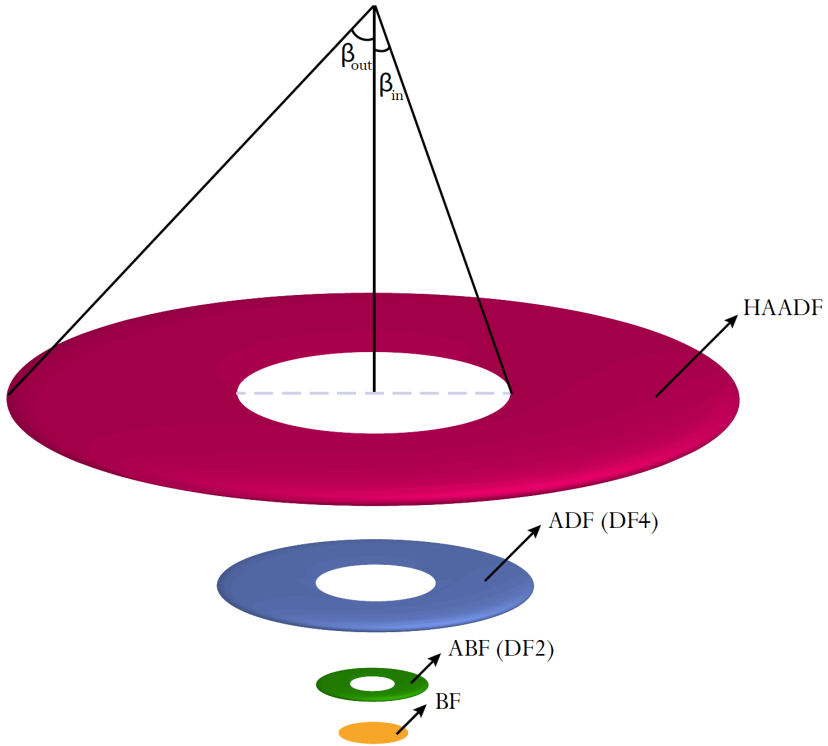

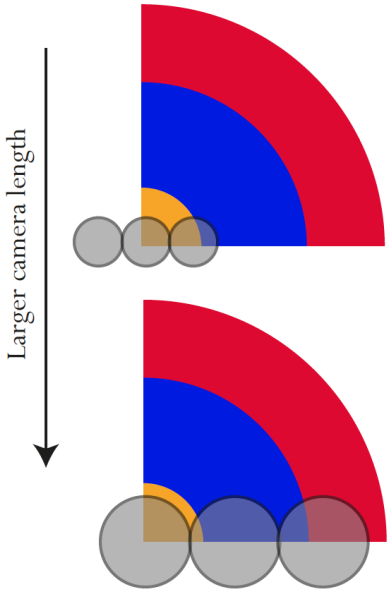

Emad Oveisi

Principles of STEM | Knowledge of angles

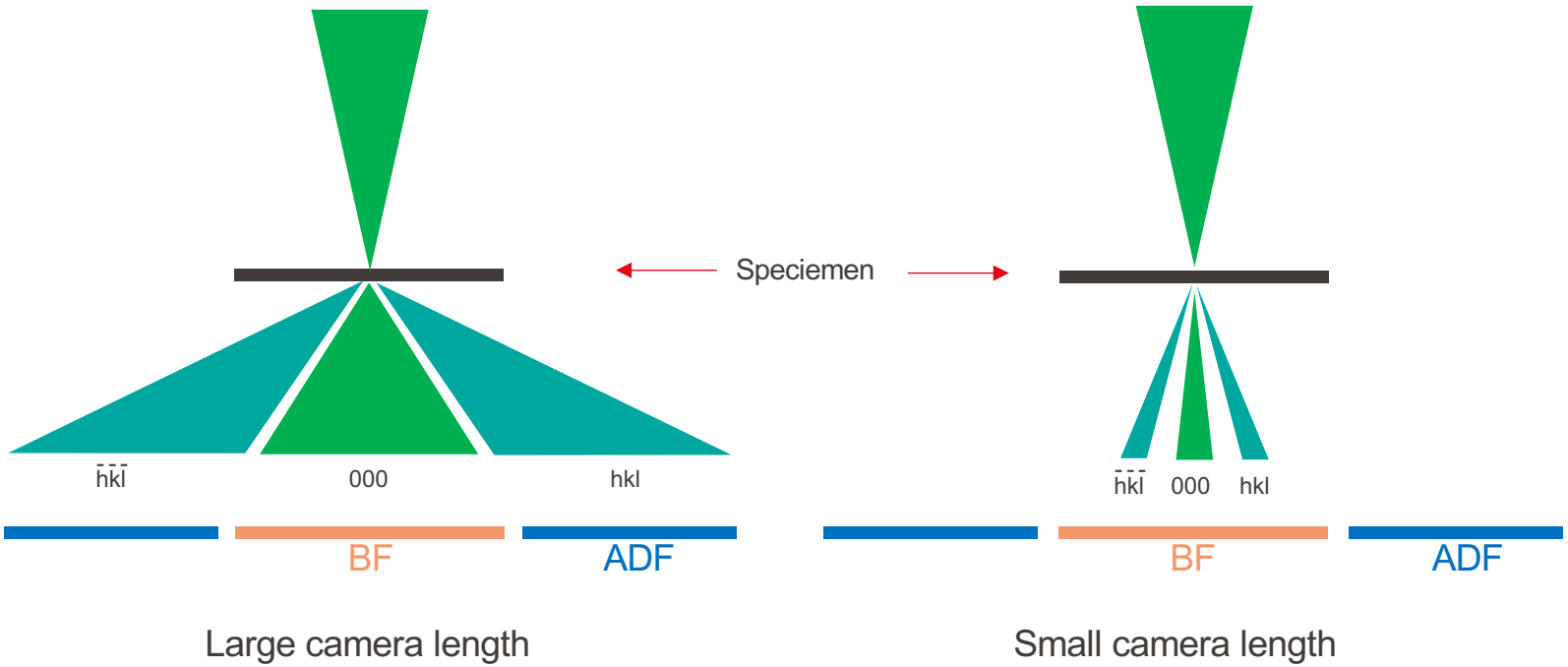

Large camera length

Small camera length

Imaging modes

Emad Oveisi

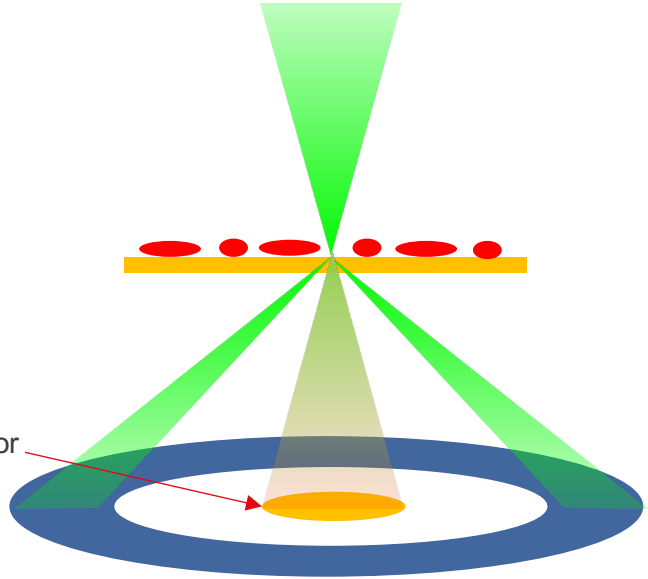

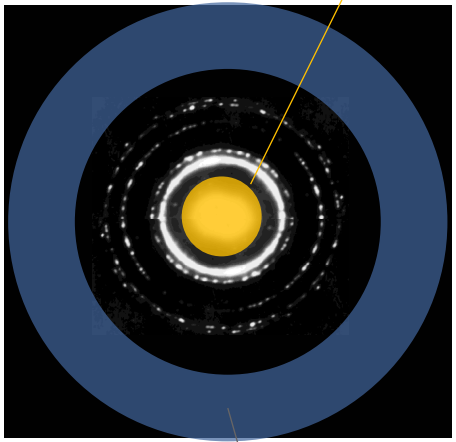

Imaging modes

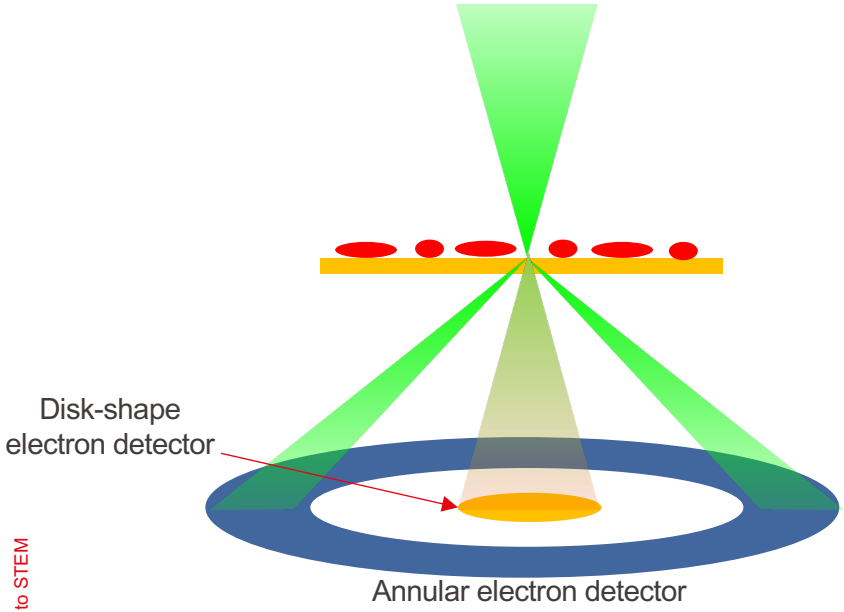

The BF detector is a solid disc that collects the direct (unscattered or low-angle scattered) beam, whose intensity varies depending on the specific point on the specimen illuminated by the probe at that moment.

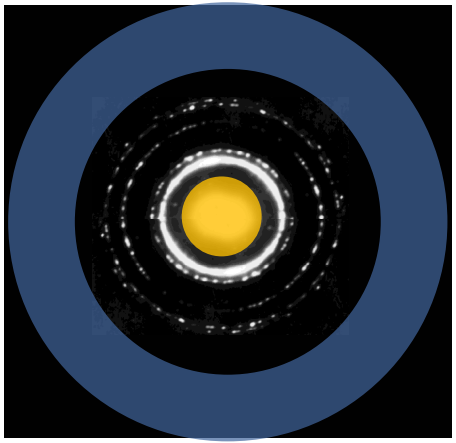

Bright-field: On axis | Electrons pass throught the sample without being scattered → Coherent imaging

Imaging modes

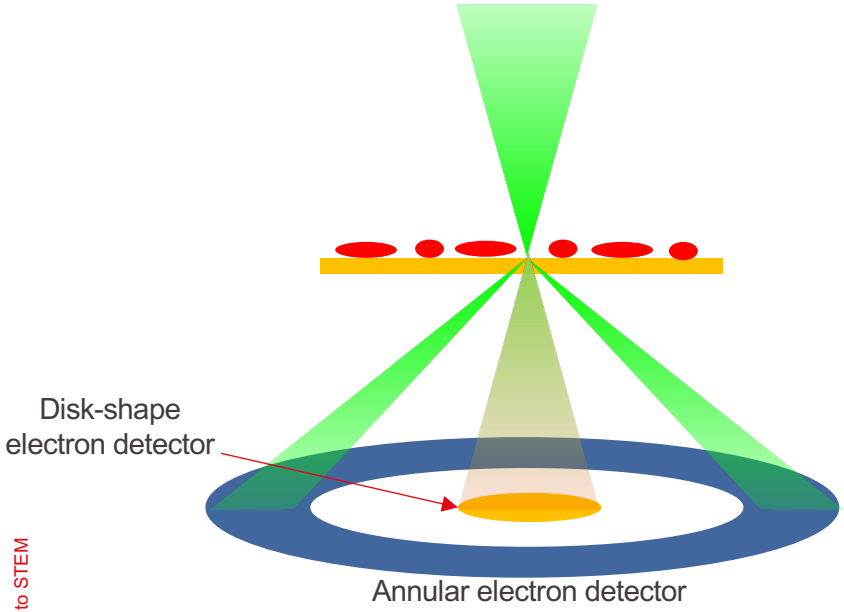

For dark-field imaging, an annular detector with inner and outer collection semi-angles defined by the camera length is used. It surrounds the BF detector and collects the electrons scattered into those angles.

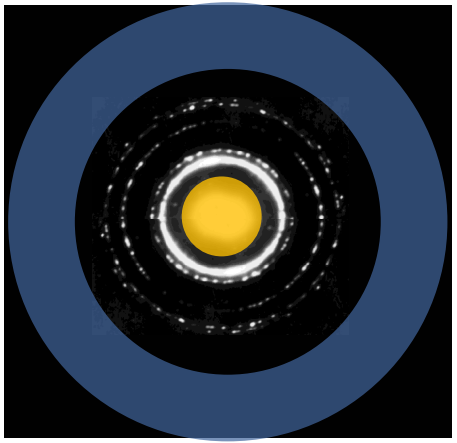

Annular dark-field: Off-axis | Electrons diffracted off axis by ineraction with the sample

Imaging modes | Annular dark-field

- Proposed by Crewe and co-workers during the early development of the modern STEM.

- The detector consists of an annular sensitive region that collects electrons scattered over a defined angular range. The radii can vary over a wide interval, but typically the inner radius is in the range of 30–100 mrad and the outer radius in the range of 100–200 mrad.

- At high scattering angles (> ~100 mrad), the compositional contrast is enhanced, and the coherent effects of elastic scattering can be neglected because the scattering is predominantly thermally diffuse. This results in **incoherent imaging**.

Imaging modes

Bright-field TEM

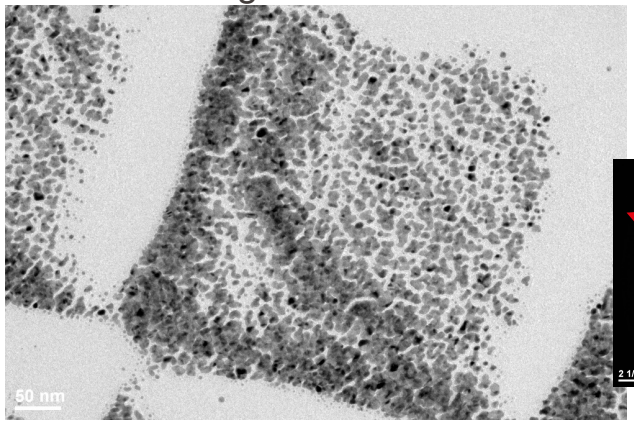

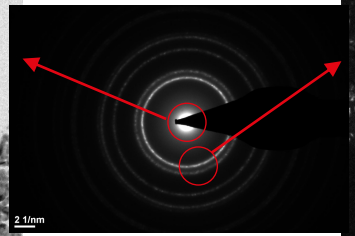

Aperture

Dark-field TEM

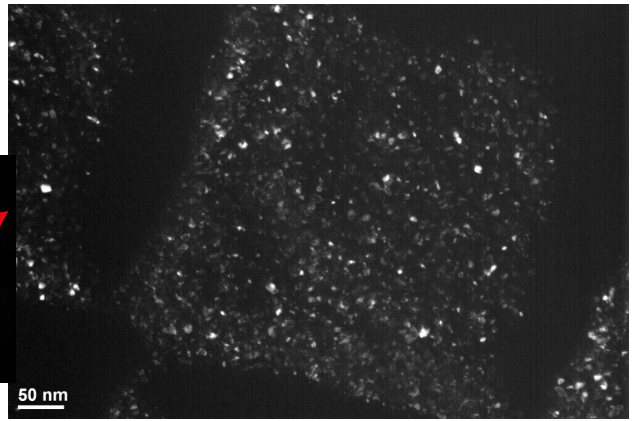

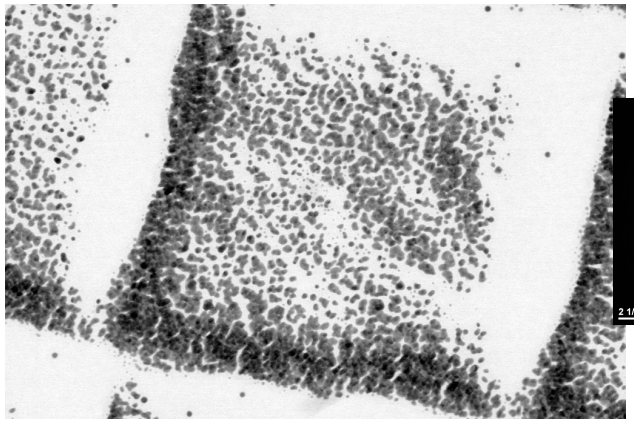

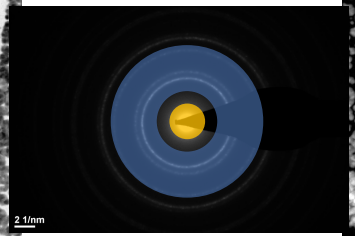

Detector

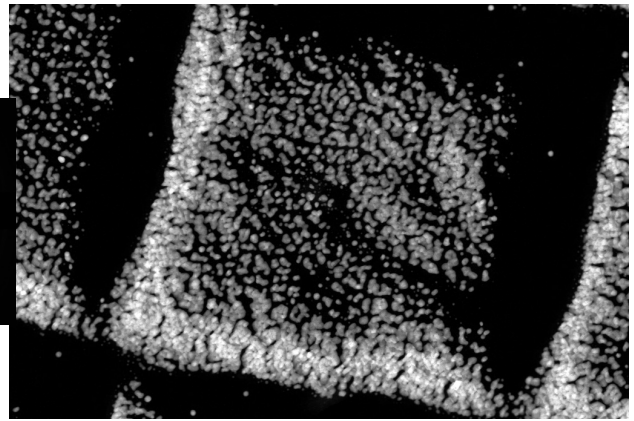

Bright-field STEM

Annular dark-field STEM

Imaging modes

ADF-STEM and DF-TEM images of a photovoltaic stack

Visible: Protocrystalline/crystalline Si interface, B-doped layer in proto-Si, voids

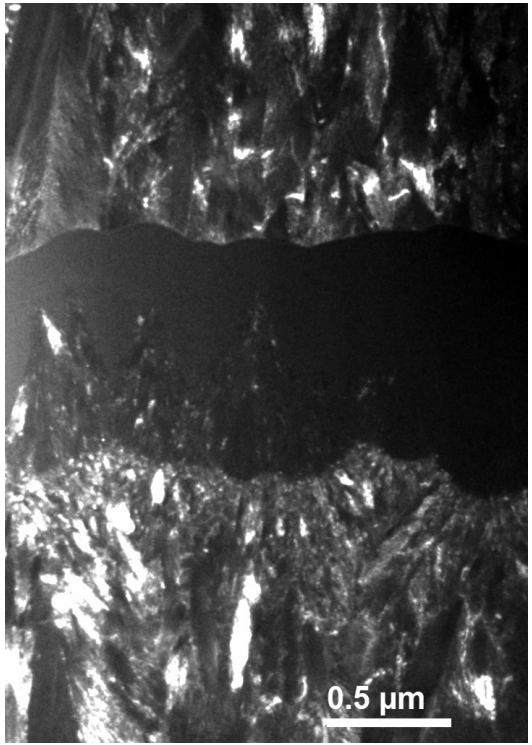

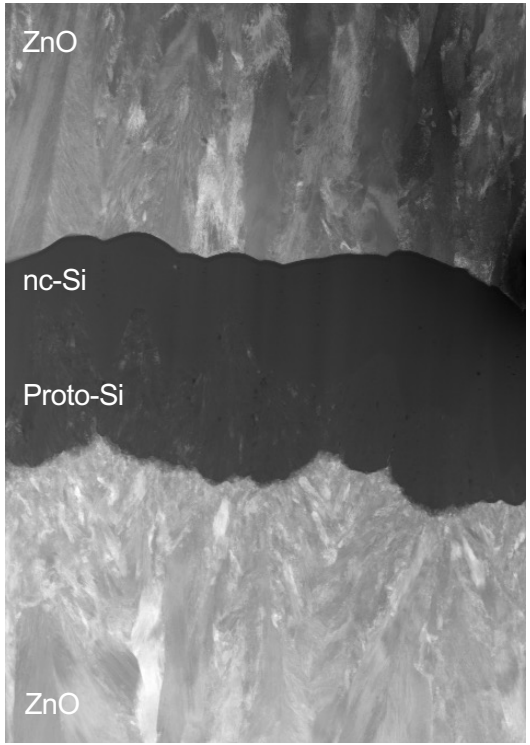

Which one is the annular dark-field STEM image?

Slide courtesy of D.T.L. Alexander, EPFL

Imaging modes

ADF-STEM and DF-TEM images of a photovoltaic stack

Visible: Protocrystalline/crystalline Si interface, B-doped layer in proto-Si, voids

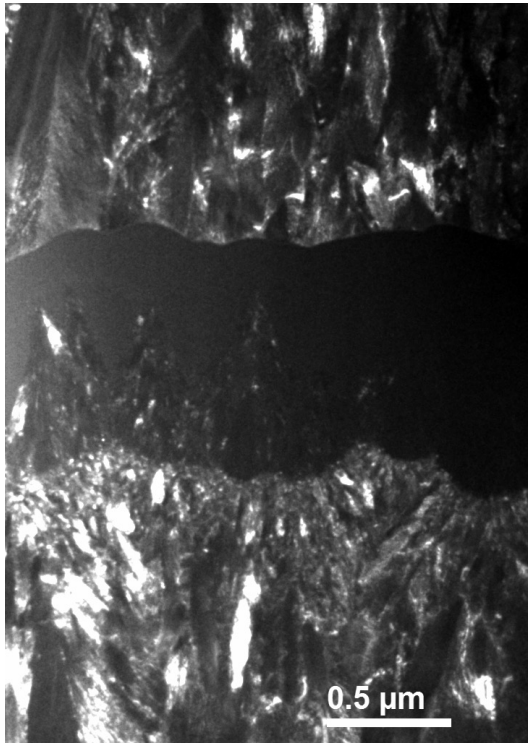

Few grains have intensity
strong contrast

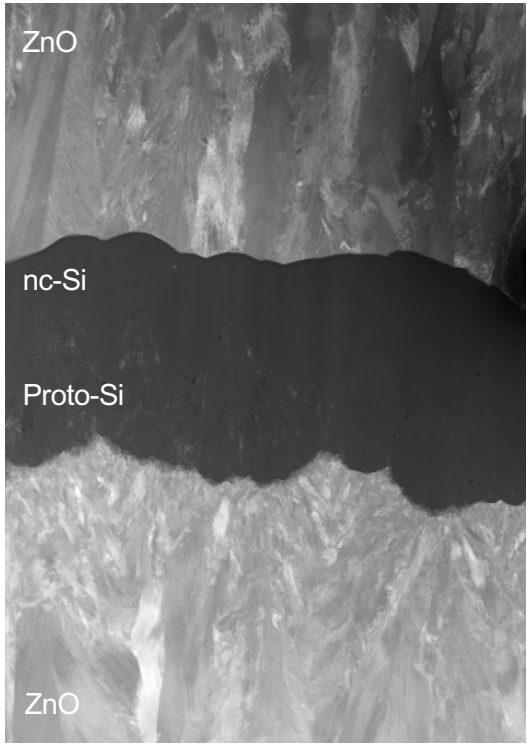

More grains have intensity
More grain visibility & less contrast

Slide courtesy of D.T.L. Alexander, EPFL

Imaging modes | High-angle annular dark-field (HAADF)

Emad Oveisi

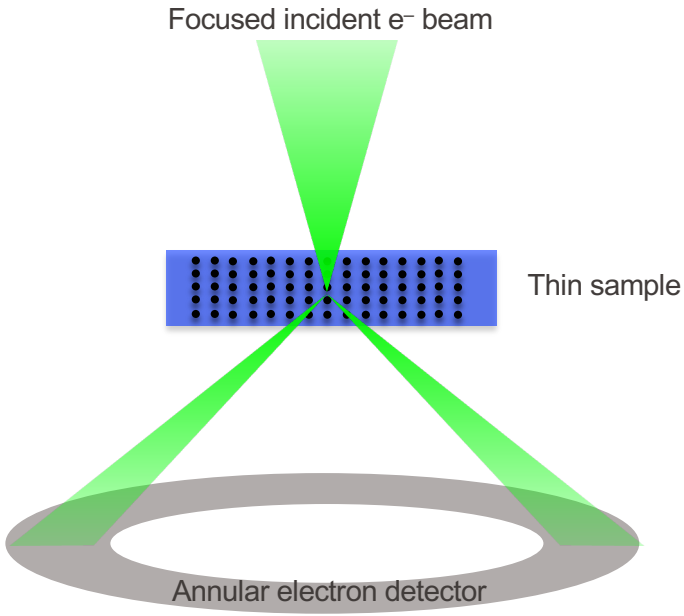

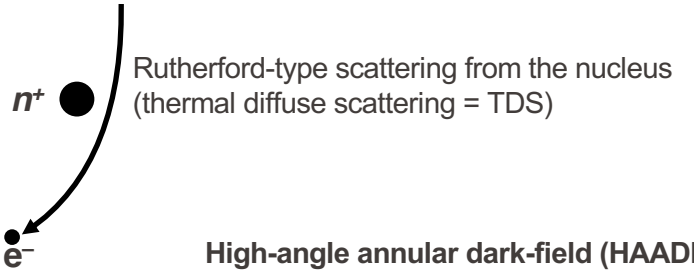

High-angle annular dark-field (HAADF) image

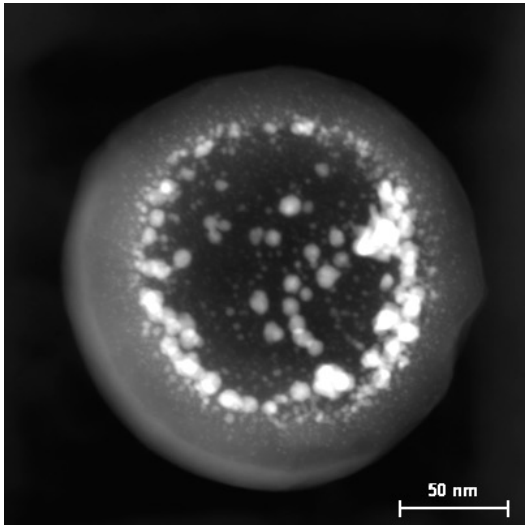

Ni-Rh catalytic nanoparticles in carbon shell

Mass/thickness contrast image

- Incoherent Rutherford-type scattering deflects transmitted e^- to high scattering angles
- A larger nucleus or a thicker specimen results in more scattering.
- The image maps intensity as a function of probe position (x,y):

  $I(x, y) \propto t * Z^{1.6-2}$, where t is the local thickness and Z is the atomic number.

Imaging modes | High-angle annular dark-field

Cs-corrected atomic resolution HAADF-STEM of perovskite interface (300 kV)

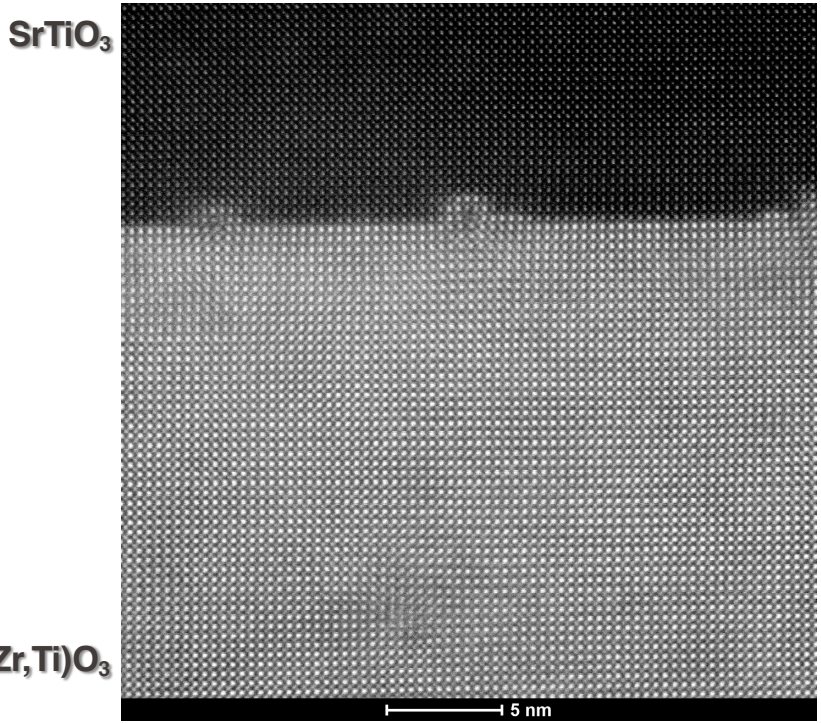

Imaging modes | High-angle annular dark-field

Cs-corrected atomic resolution HAADF-STEM of perovskite interface (300 kV)

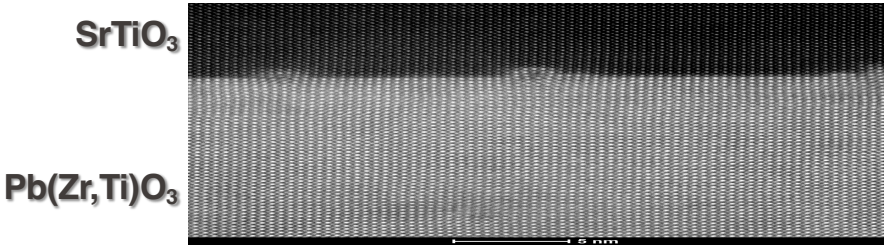

Imaging modes | High-angle annular dark-field

Emad Oveisi

Individual Pt atoms in a metallosupramolecular polymer

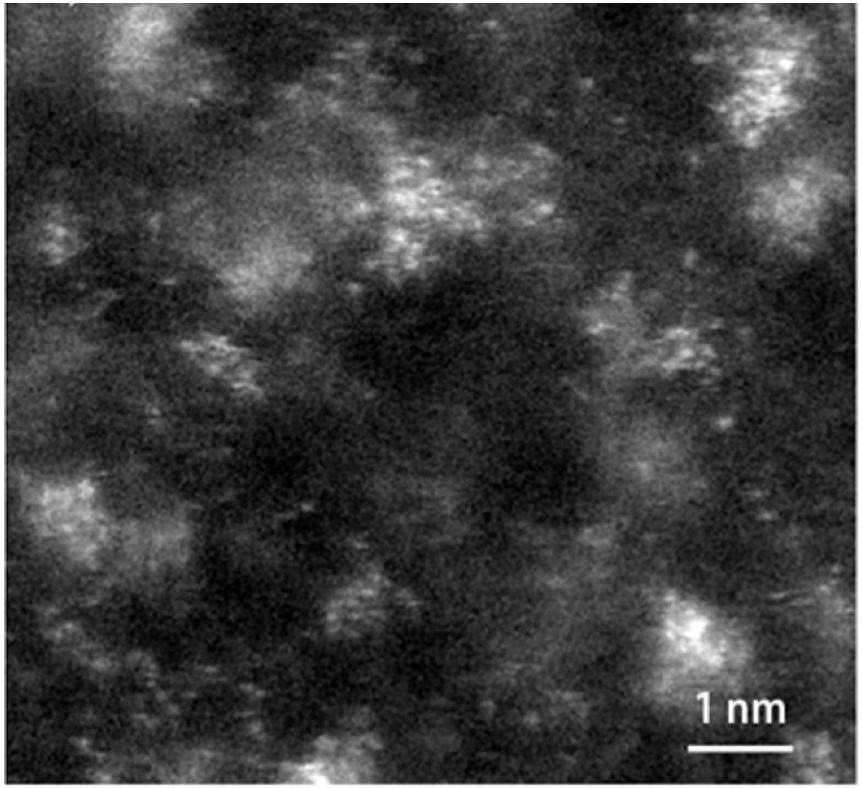

In collaboration with Adolphe Merkle Institute.
Olaeche *et al.*, JACS 2020.

Imaging modes | High-angle annular dark-field

Emad Oveisi

In / Ga multilayer

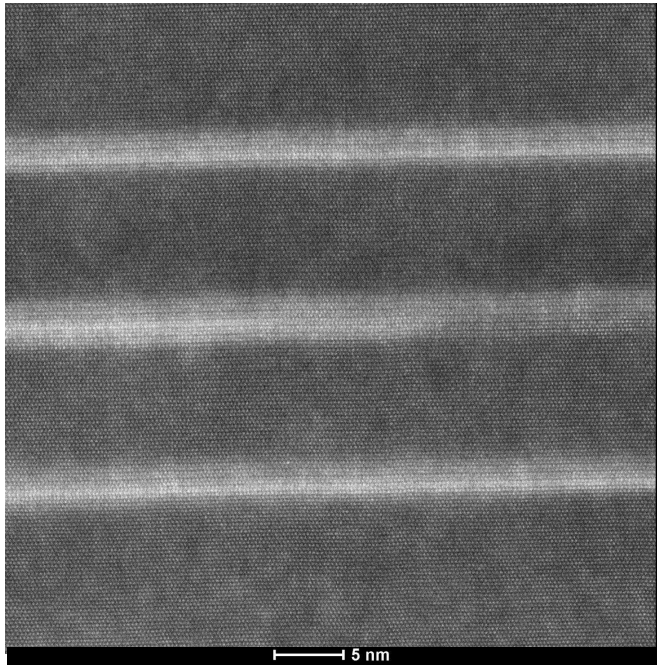

Evaluated map of the In concentration

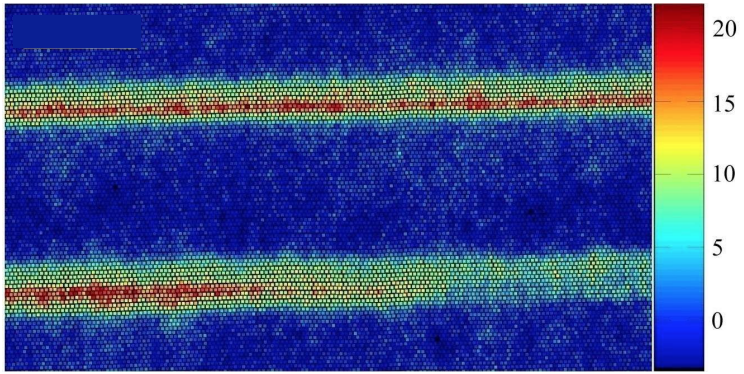

Quantitative STEM allows measurement of composition

Requires detector calibration

Imaging modes | High-angle annular dark-field

Emad Oveisi

Ag cluster embedded in an Al matrix together with the number of Ag atoms per column

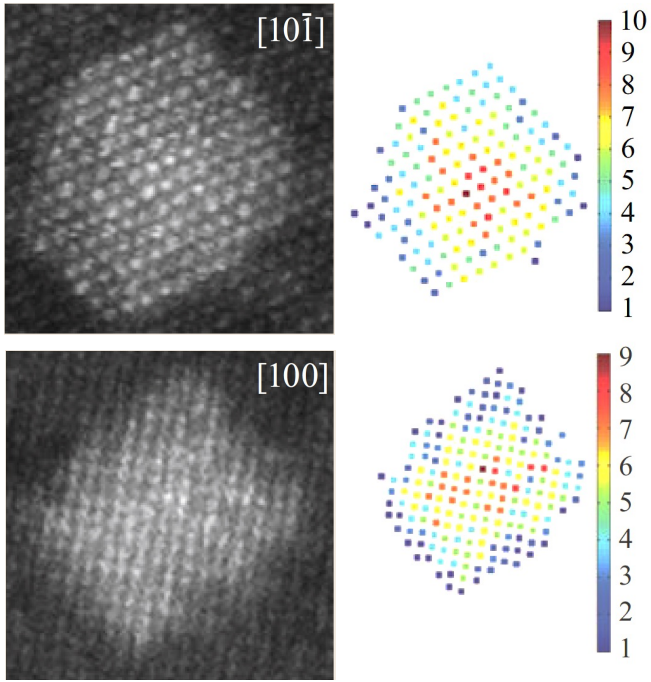

Computed 3-D reconstruction of the cluster viewed along three different directions

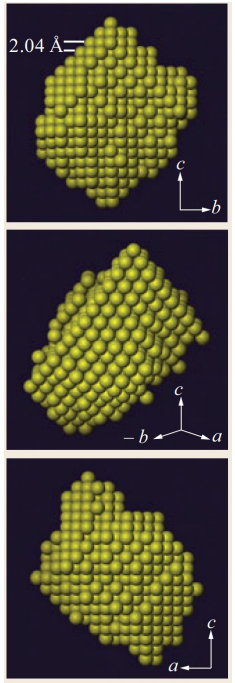

Atom counting implies precise detector calibration and assumptions about the sample

S. Van Aert *et al.*, Nature 470, 374– 377 (2011).

Imaging modes | High-angle annular dark-field

Example : Variation of the intensity according to the number of graphene layers

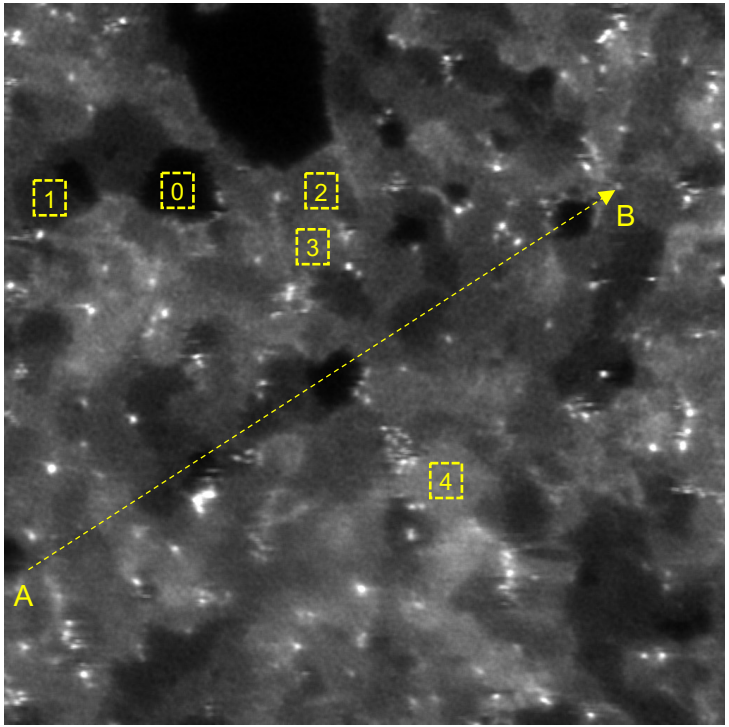

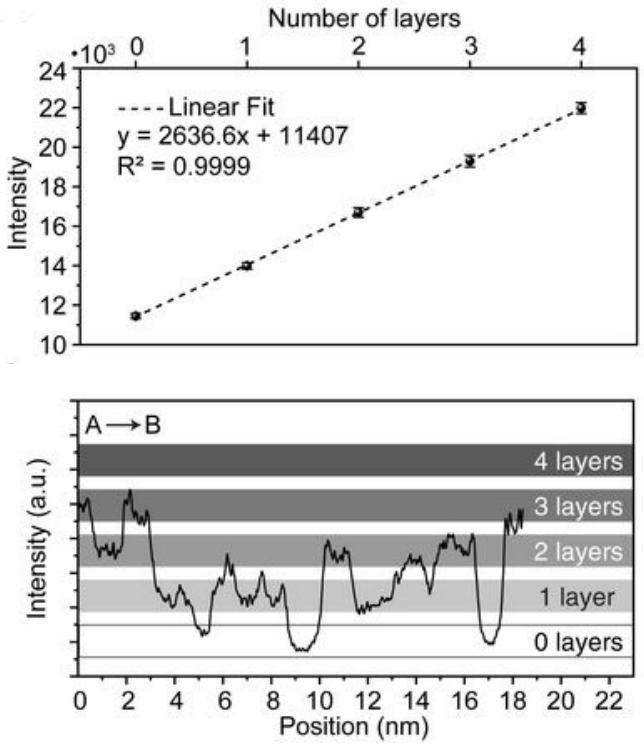

In collaboration with LAS, EPFL.
Luis Francisco Villalobos *et al.* PNAS 2021

Imaging modes | Effect of camera length

High camera lengh

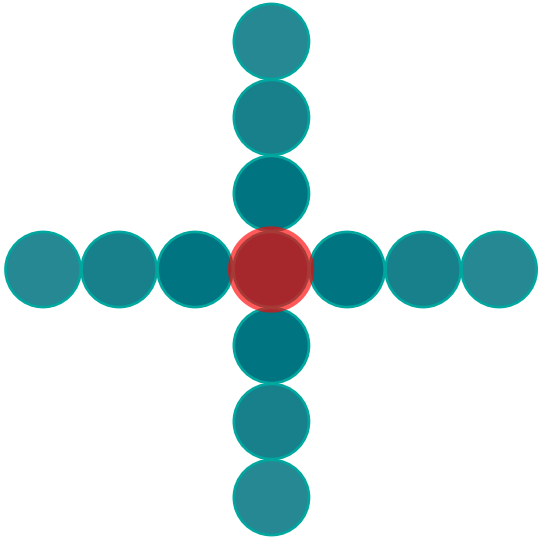

Direcly tranmistted disk on the solid disk detector
→ BF-STEM image

Low camera lengh

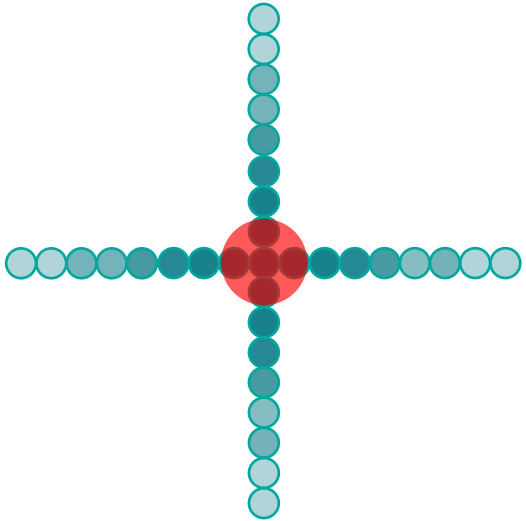

Both direct and diffracted disks
on the the solid disk detector

Imaging modes | Effect of camera length

High camera lengh

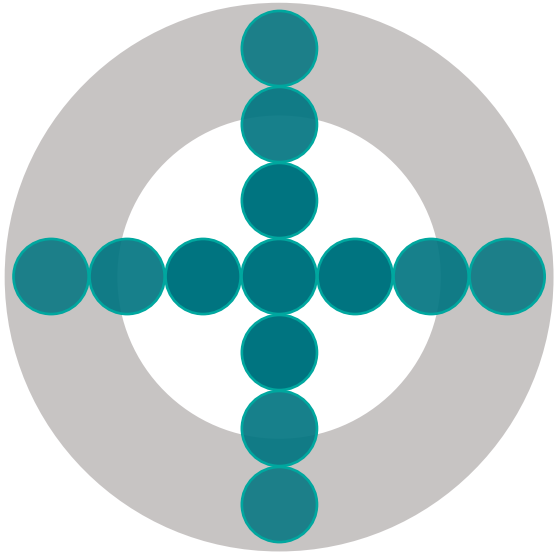

Dominant diffraction contrast

Low camera lengh

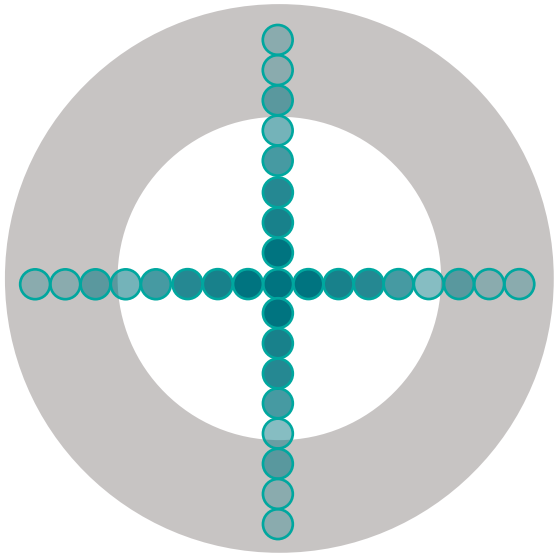

Dominant Z-contrast (TDS)

Imaging modes | Effect of camera length

High camera lengh

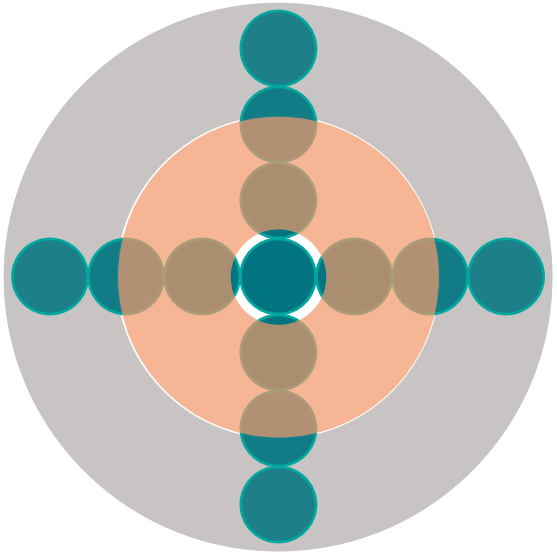

Mixed diffraction and Z-contrast → MAADF

Pure diffraction contrast → LAADF

Low camera lengh

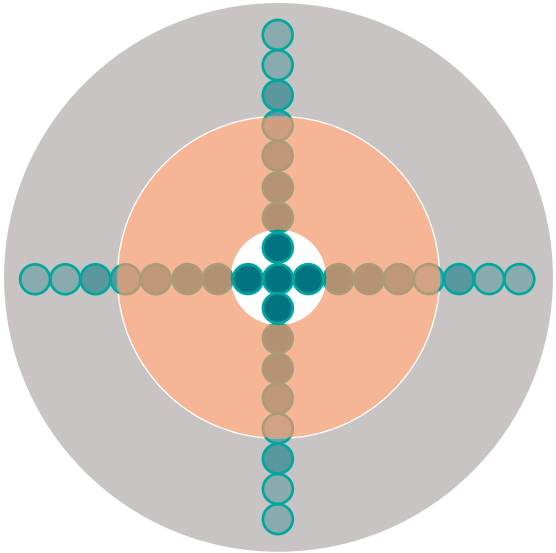

Z-contrast image → HAADF

Mixed diffraction and Z-contrast → MAADF

Imaging modes | Effect of camera length

High camera lengh

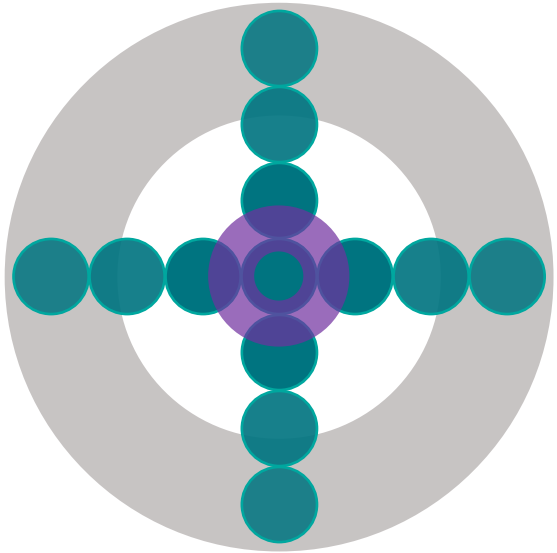

Mixed diffraction and Z-contrast → MAADF

Annular bright-field (ABF) image

Low camera lengh

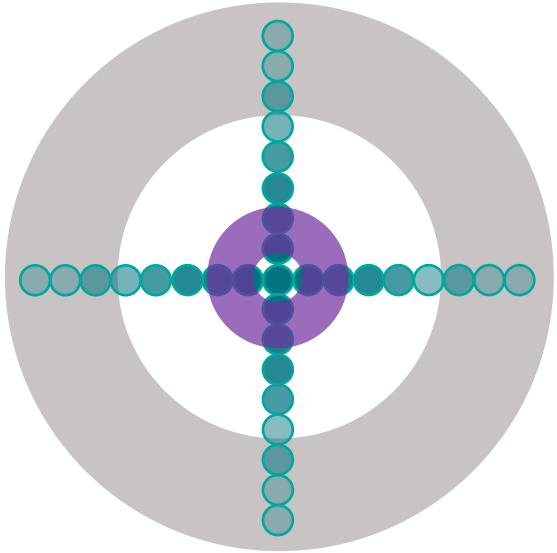

Z-contrast image → HAADF

Pure diffraction contrast → LAADF

Imaging modes | Effect of camera length

High camera lengh

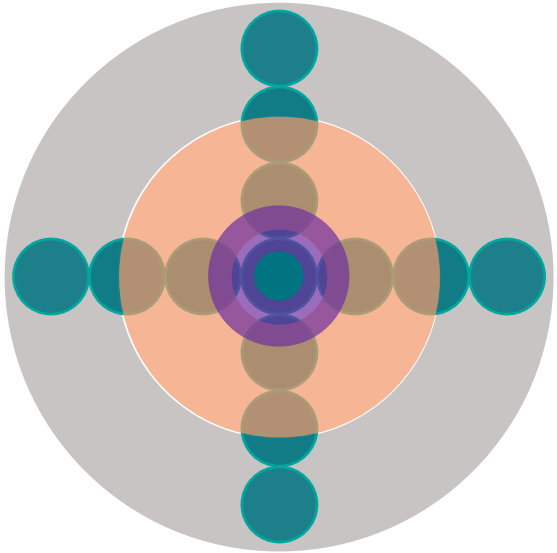

Mixed diffraction and Z-contrast → MAADF
Pure diffraction contrast → LAADF
Annular bright-field (ABF) image

Low camera lengh

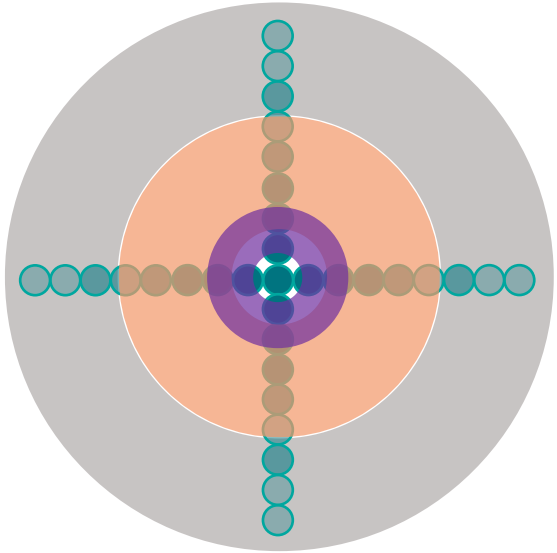

Z-contrast image → HAADF
Mixed diffraction and Z-contrast → MAADF
Pure diffraction contrast → LAADF

Imaging modes | Low-angle annular dark-field

Emad Oveisi

Example: Variation of defect contrast with camera length in γ / γ' region of Ni-superalloy

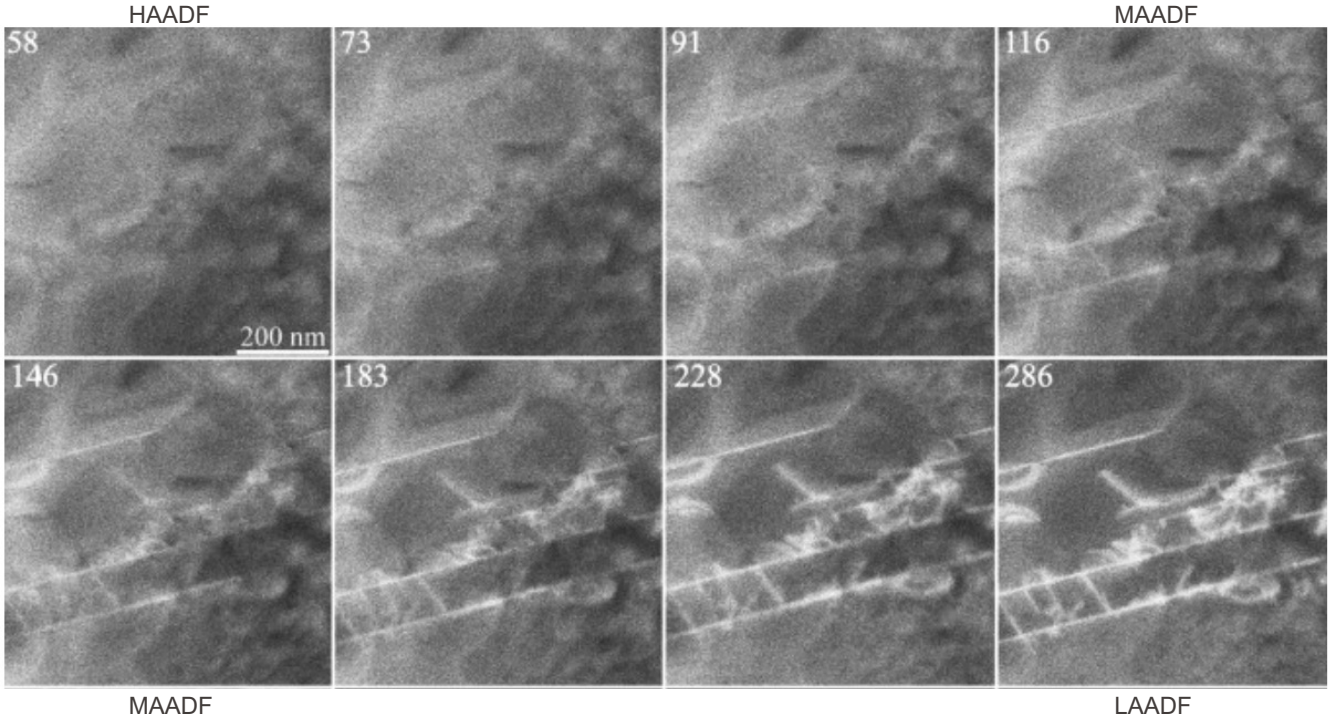

Philips *et al.*, Ultramicroscopy 2012.

Imaging modes | Medium-angle annular dark-field

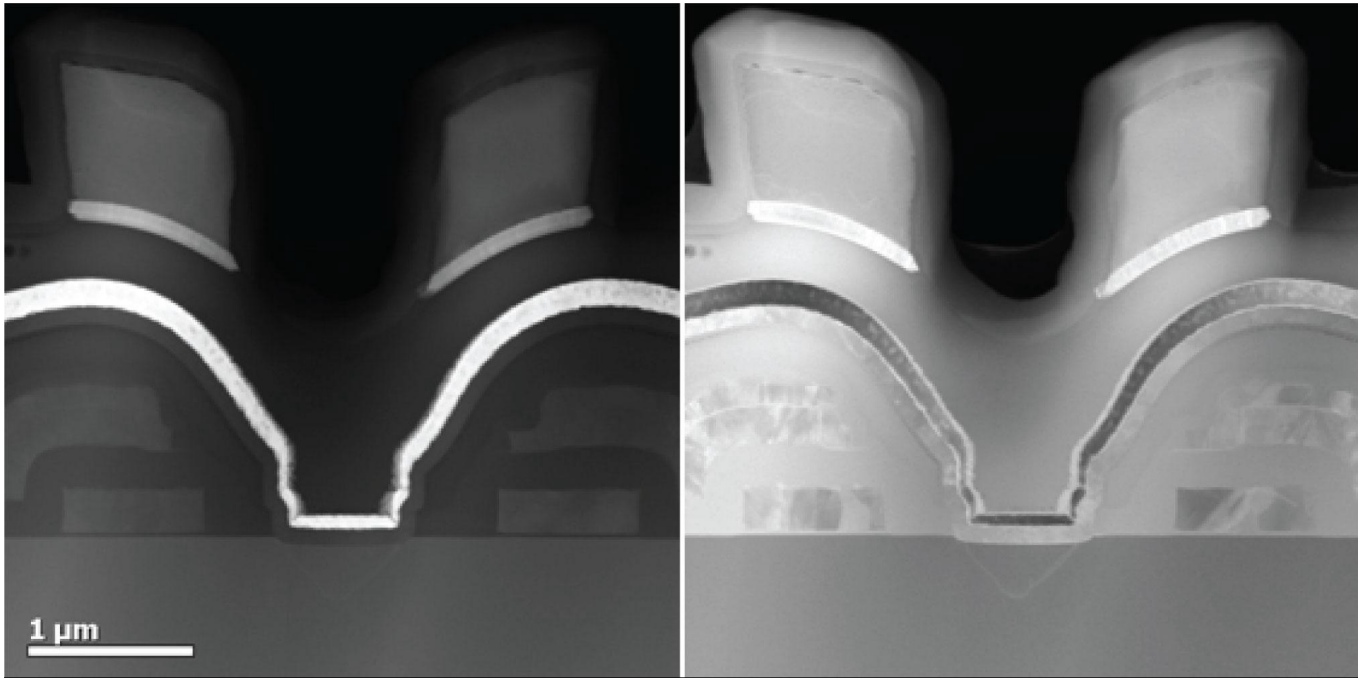

Jointly acquired HAADF and MAADF signals

The HAADF signal (left) provides contrast that can be easily interpreted in terms of the mass-thickness of the material, while the diffraction-contrast MAADF signal (right) reveals fine structural details.
This is made possible by the optimized detector geometry.

https://www.gatan.com/products/tem-imaging-spectroscopy/advanced-stem-detectors

Emad Oveisi

Imaging modes | Medium-angle annular dark-field

Example: Doped graphene, BN monolayer – C_S STEM

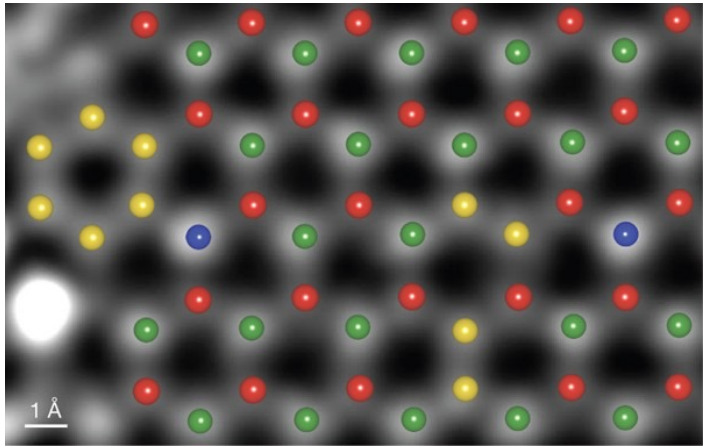

Low kV is essential to prevent knock-on damage; here 60 kV used.

As λ increases aberration correction is even more important for obtaining atomic resolution.

Medium-angle ADF gives intensity I $\propto Z^{1.7}$ but with increased signal intensity for low-Z elements compared to true HAADF image. This intensity is needed for imaging single atoms (here β = 58–200 mrad)

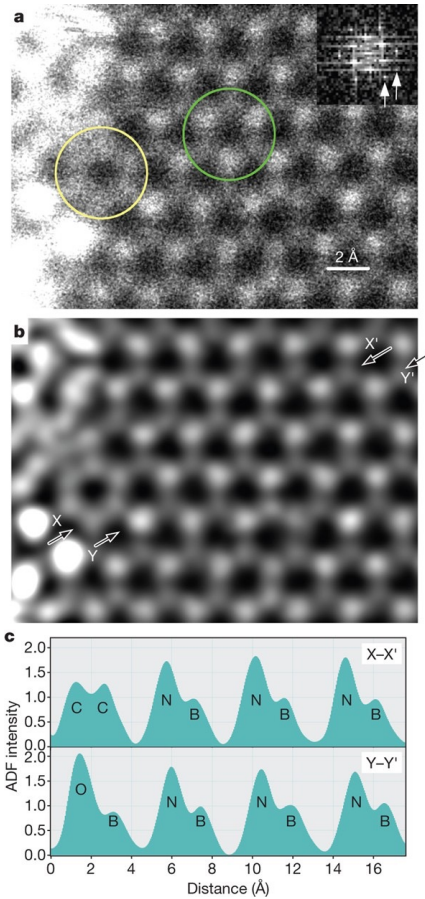

Krivanek,*et al.* Nature **464** (2010).

Imaging modes | Coherent vs incoherent image

- **Coherent:** Phase-sensitive, diffraction-dependent

Characteristics:

- ✓ Coherent artifacts (fringes, contrast reversals) can appear
- ✓ Interference produces contrast;
- ✓ Sensitive to diffraction and lattice structure
- ✓ Contrast depends on thickness, orientation, and defocus
- ✓ Possible contrast reversal with focus and thickness

Examples:
Bright-field, Phase-contrast TEM, LAADF-STEM

- **Incoherent:** Phase-insensitive, intensity directly reflects scattering cross-section

Characteristics:

- ✓ Camera-like characteristic:
  Atoms in the image appear sharp when focused and blur when defocused.
- ✓ Less sensitive to diffraction
- ✓ Image intensity directly related to mass-thickness
- ✓ Directly interpretable contrast
- ✓ No contrast reversal with focus

Examples:
MAADF- and HAADF-STEM

Example: Si <110>

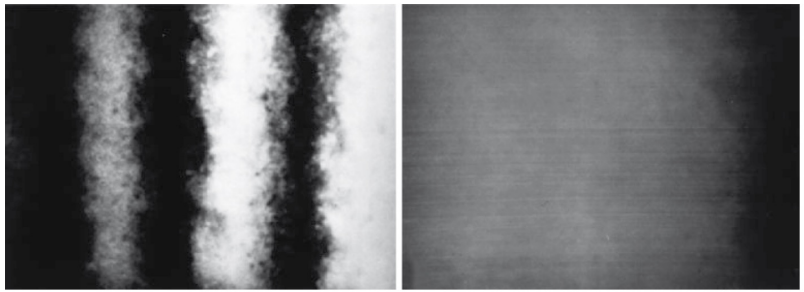

BF-STEM: Thickness fringes visible
→ Coherent

Z-contrast image
→ Incoherent

Ultramicroscopy, 37 (1991), pp. 14-38

Imaging modes | Coherent vs incoherent image

Emad Oveisi

BF-TEM

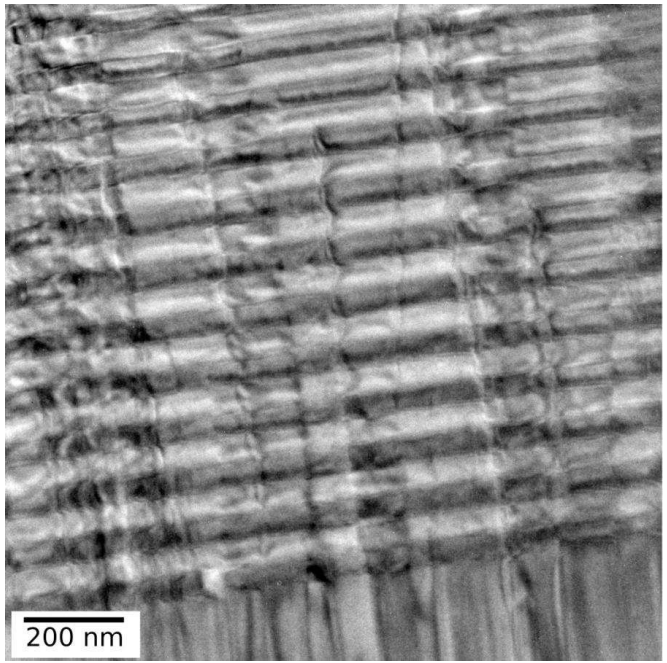

Contrast due to strain and diffraction effects

HAADF-STEM

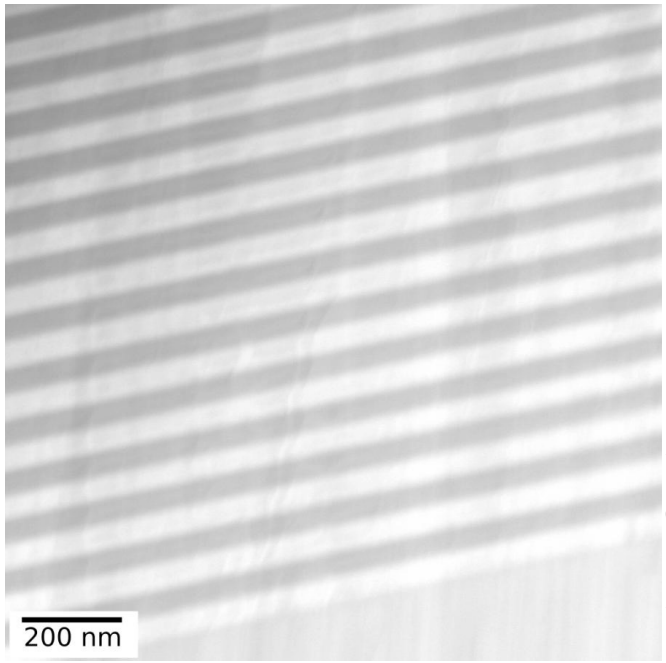

Contrast determined by atomic number

Imaging modes | Coherent vs incoherent image

Emad Oveisi

Example: Images of a Ge film grown epitaxially on Si

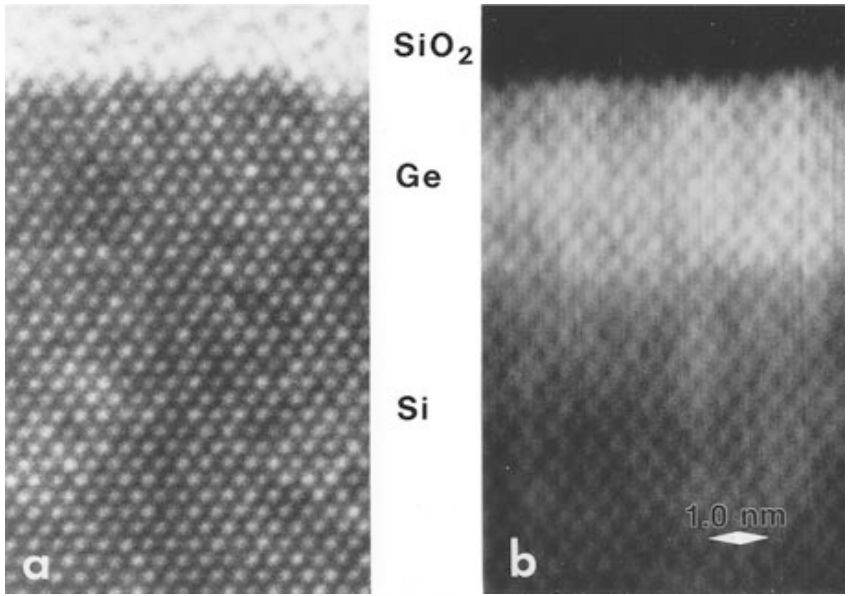

Conventional TEM image

Z-contrast image clearly delineating the Ge layer

Ultramicroscopy, 37 (1991), pp. 14-38

Imaging modes | Coherent vs incoherent image

Emad Oveisi

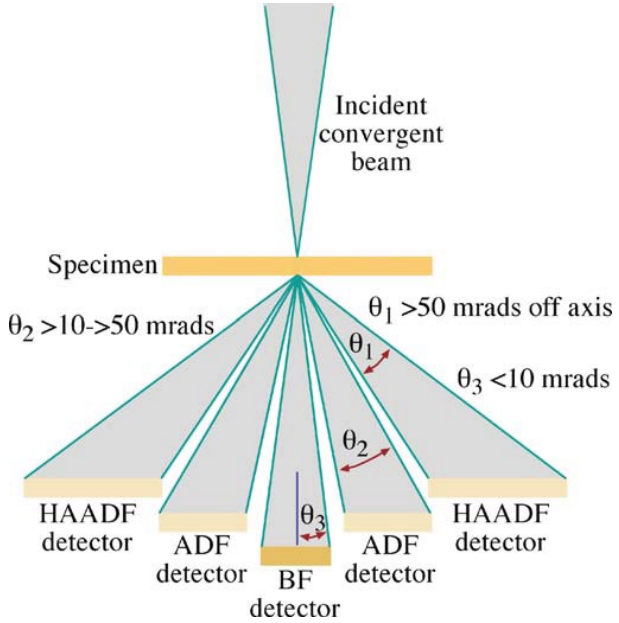

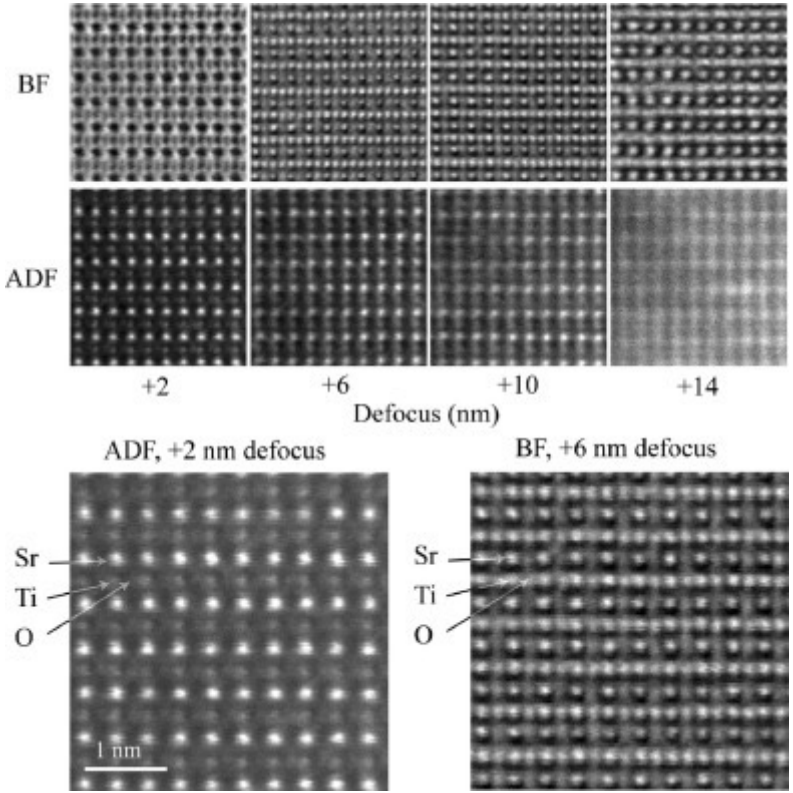

BF | On-axis → Coherent : Contrast reversal with focus/thickness

ADF | Off-axis → Incoherent (no phase relation with the inceident beam) : No Contrast reversal with focus/thickness

Pennycook S.J., Ultramicorscopy (2017) 180, 22-33.

Imaging modes | Annular bright-field

- HAADF not useful for imaging light atoms in a sample with heavy atoms because the contrast depends strongly on atomic number.
- BF imaging has some disadvantages for imaging light atom columns, similar to phase-contrast HR-TEM imaging.
- Harald Rose's annular bright-field (ABF) imaging (with aberration correction), where central part of BF detector is obscured, solves these problems.
- ABF produces a phase-contrast image; however, because it effectively sums signals from many point detectors—each with a different CTF—the resulting contrast is **largely incoherent over a wide range of thicknesses and defocus values**.
- Typically, the collection angle extends from half the probe convergence angle to the the full probe angle. For instance, for α = 22 mrad, one would use β = 11–22 mrad

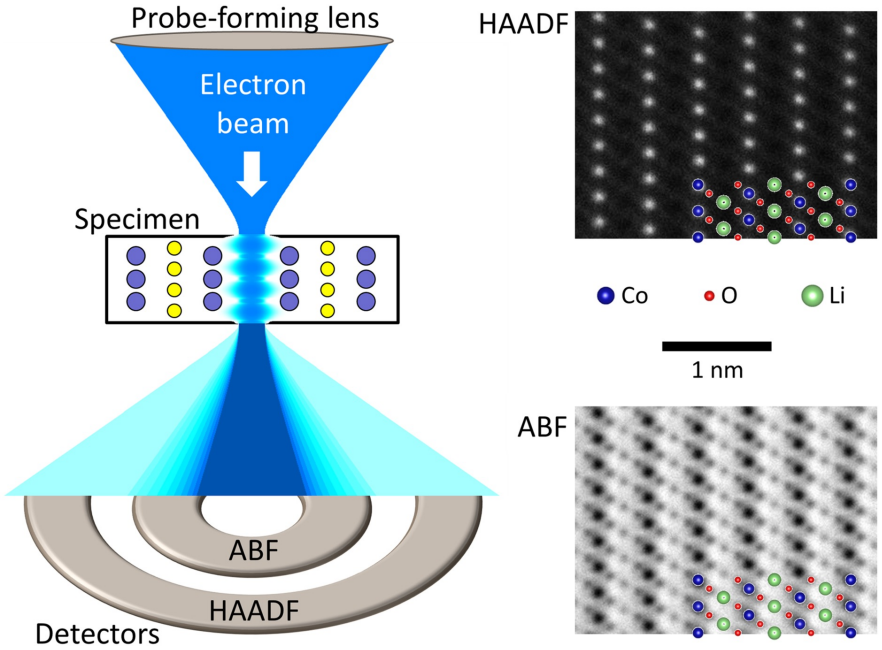

Low-Z and high-Z atoms can be seen clearly in the same image.

Findlay *et al.*, Microscopy **66** (2017).

Imaging modes | Annular bright-field

Simple theory: Channelled electrons scattered mostly into centre of BF detector by light columns giving some dark ABF contrast.

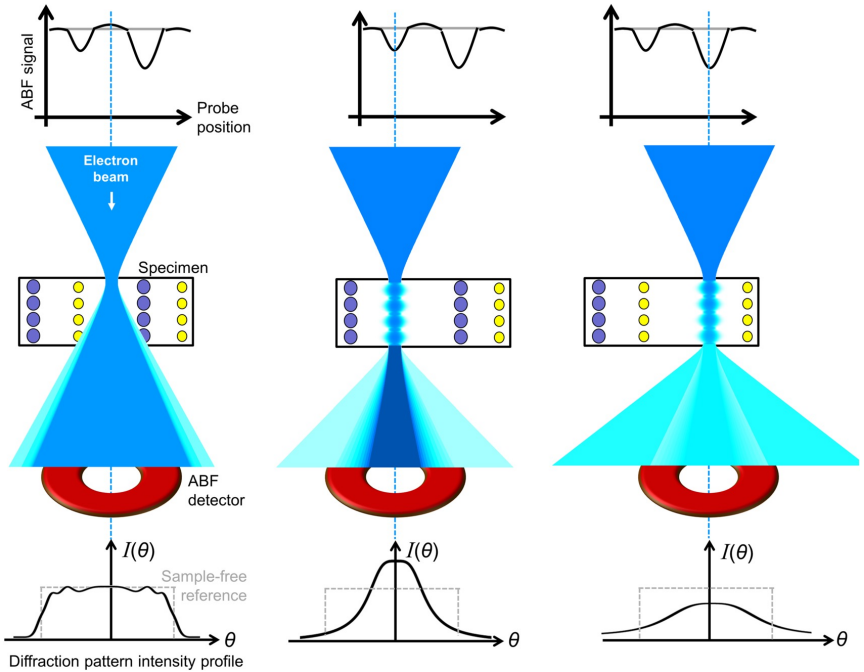

Example: $(Ba_xSr_{1-x})TiO_3$

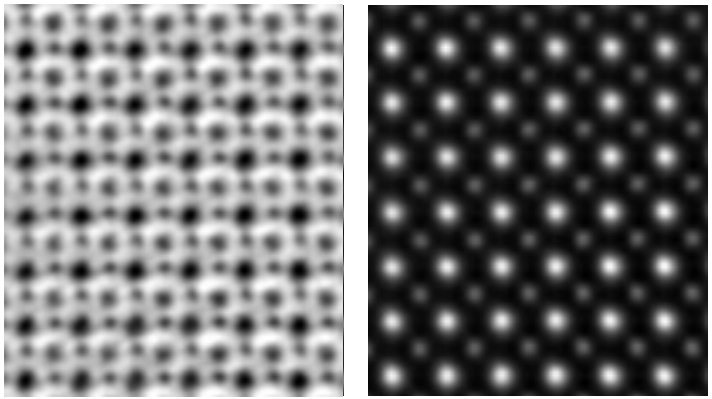

ABF HAADF

Scattered more strongly to diffracted beams by heavy columns giving darker ABF contrast. Off column little scattering, so brighter ABF contrast.

Findlay *et al.*, Microscopy **66** (2017).
Bencan and Oveisi et al. Nat. Comm. (2021).

Shadow image | Perfect lens

Assuming perfect optics, overfocus condition

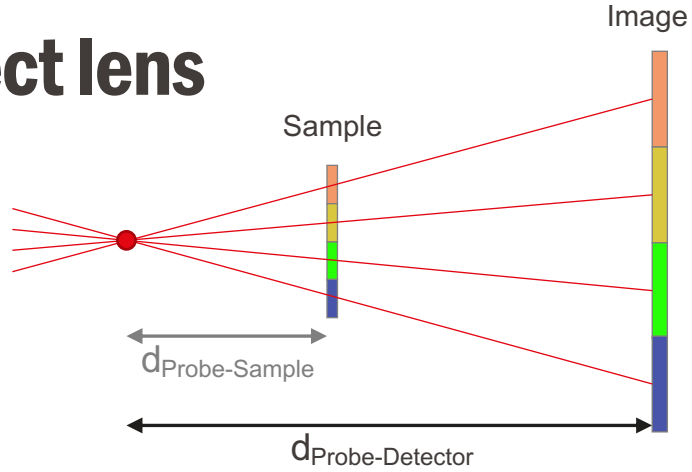

$$\text{Magnification} = \frac{d_{Probe\text{-}Detector}}{d_{Probe\text{-}Sample}}$$

At underfocus the image will magnify, but inverted

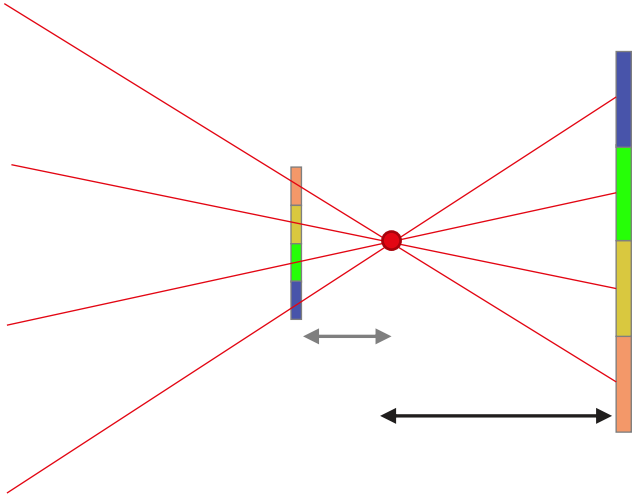

Shadow image | Real lens

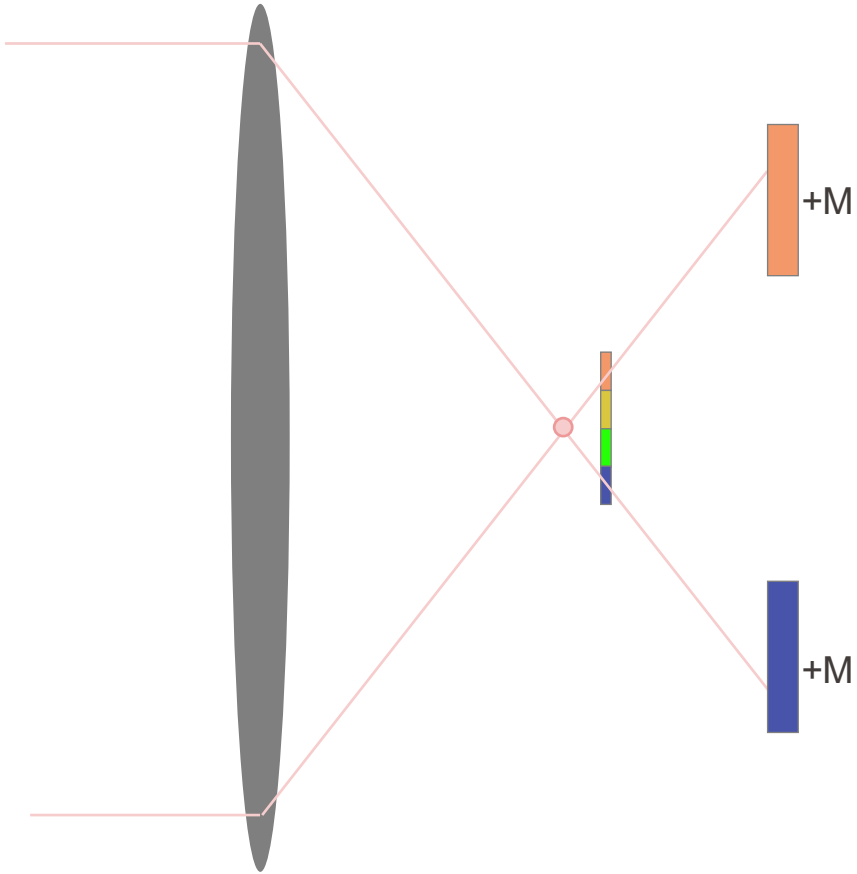

Emad Oveisi

Shadow image | Real lens

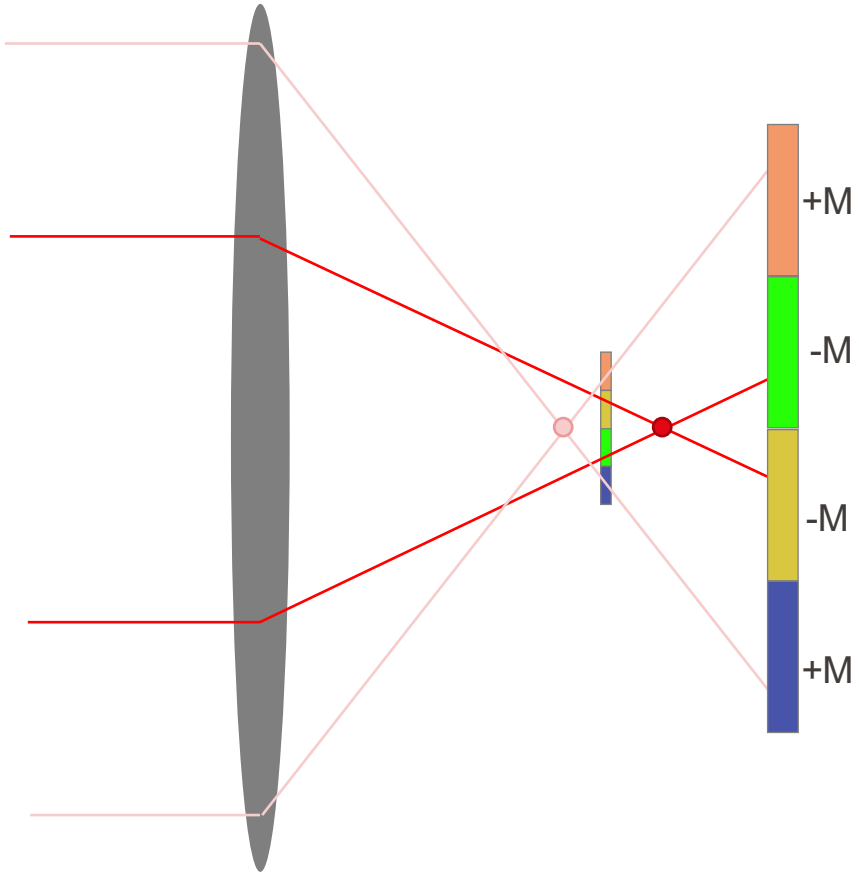

Emad Oveisi

Shadow image | Real lens

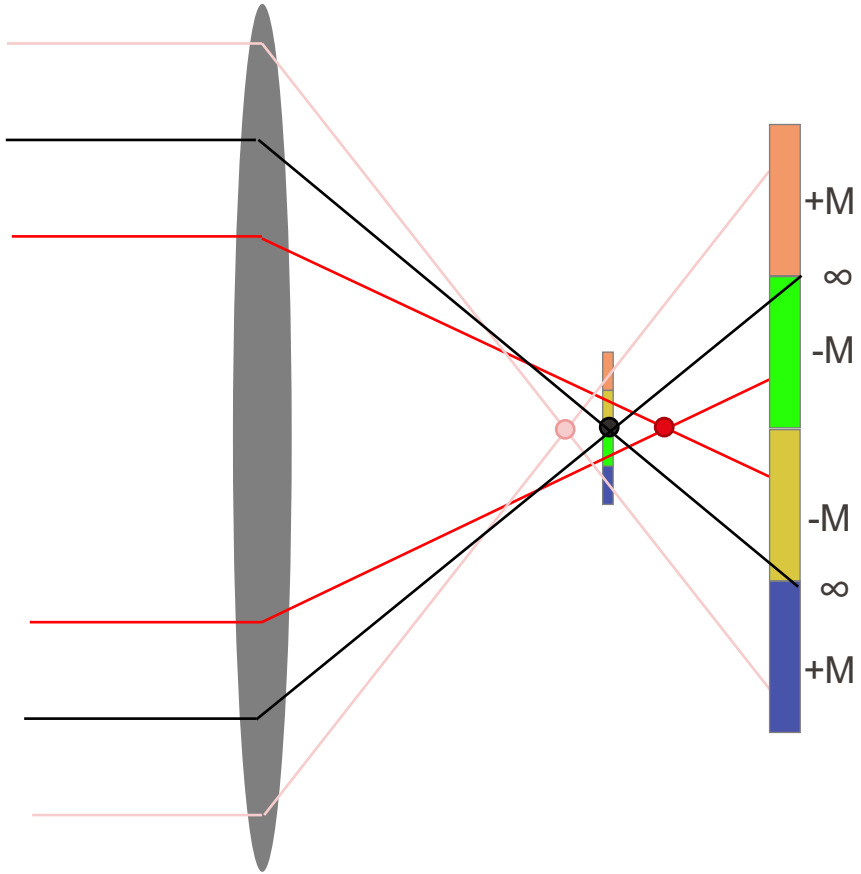

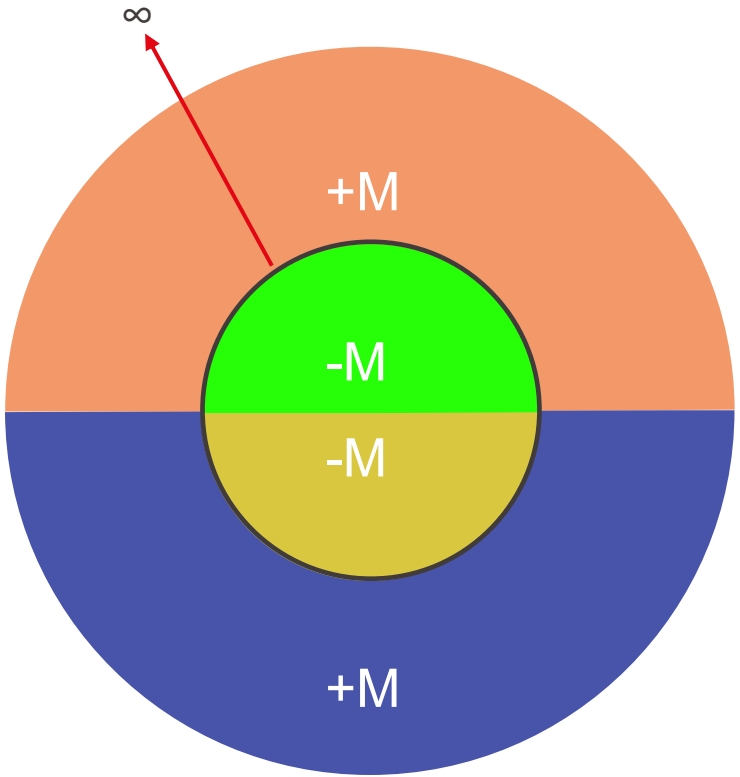

Emad Oveisi

Shadow image | Real lens

In the presence of spherical aberaration, for deocus Δ and wavevektor **k,** magnifiacation M' is:

$$M' = \frac{M}{1 + C_s\lambda^2|k|^2/\Delta}$$

In 1-D infinite magnification occurs at defocus $\Delta = -\lambda^2 C_s\,|k|^2$ or $|k|^2 = \frac{-\Delta}{\lambda^2 C_s}$

In 2-D there are two critical angles for which raidal and circumferential magnifications are equal to infinity:

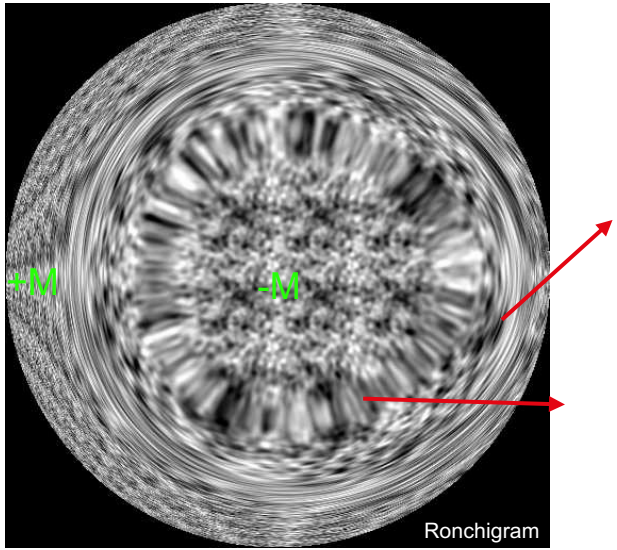

Azimuths

Radii

$|k|^2 = \frac{-\Delta}{\lambda^2 C_s}$ Circumferential

$|k|^2 = \frac{-\Delta}{3\lambda^2 C_s}$ Radial

Different Δ if there is astigmatism

The more defocus, the bigger the region in the centre which is inverted

*J.M. Cowley, Journal of Electron Microscopy Technique **3** (1986) 25.*

Shadow image | Real lens

Emad Oveisi

The more defocus, the bigger the region in the centre which is inverted

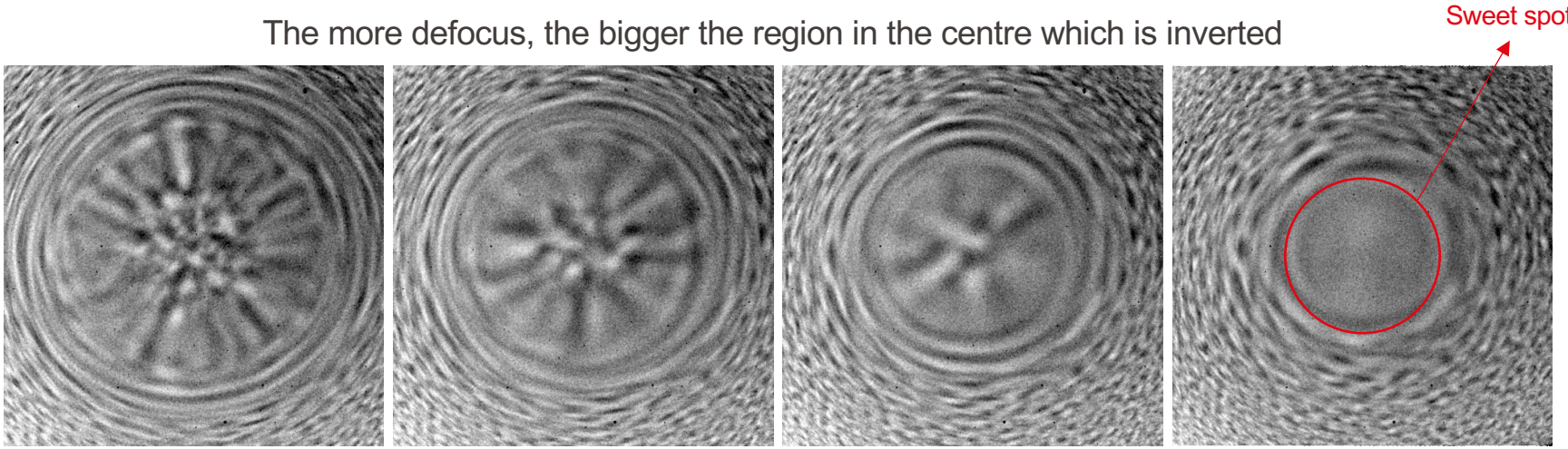

-700 nm | -450 nm | -250 nm | Optimum defocus

In practice:

- Reduce under-focus until infinite-magnification rings are of minimum diameter
  → Optimum defocus (c.f. Scherzer defocus in HR-TEM)
- Fit probe-forming aperture to the “sweet spot” region of constant phase within this

Shadow image | Real lens

Emad Oveisi

Different Δ if there is astigmatism → Eliptical Roncgigram instead of round

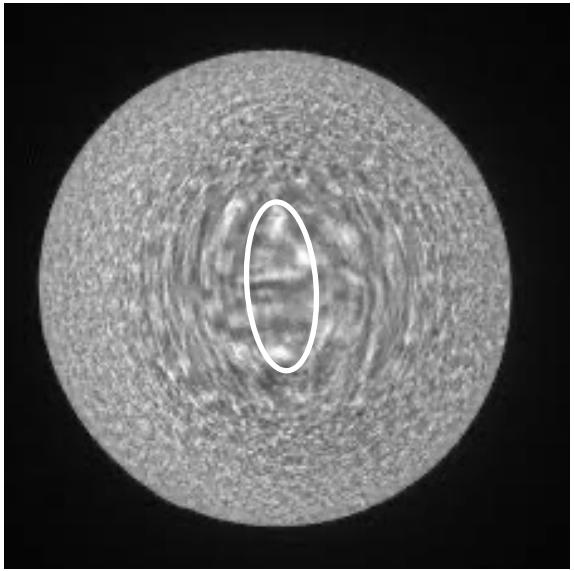

With astigmatims

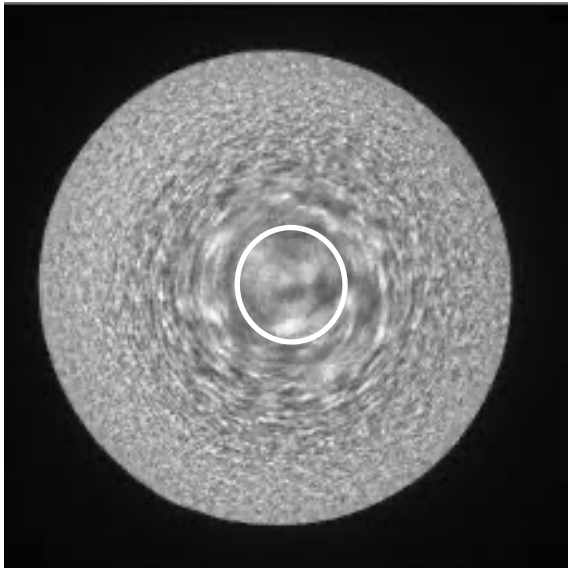

Astigmatims corrected

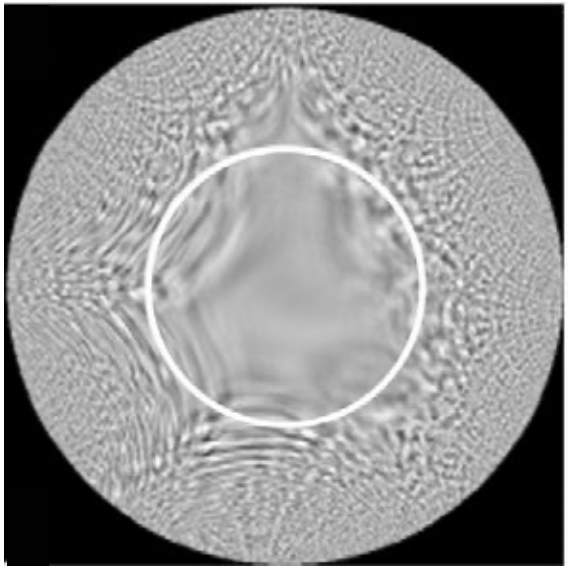

Cs corrected

Shadow image | Cs-Corrected

Cs correction increases the size of the sweet spot

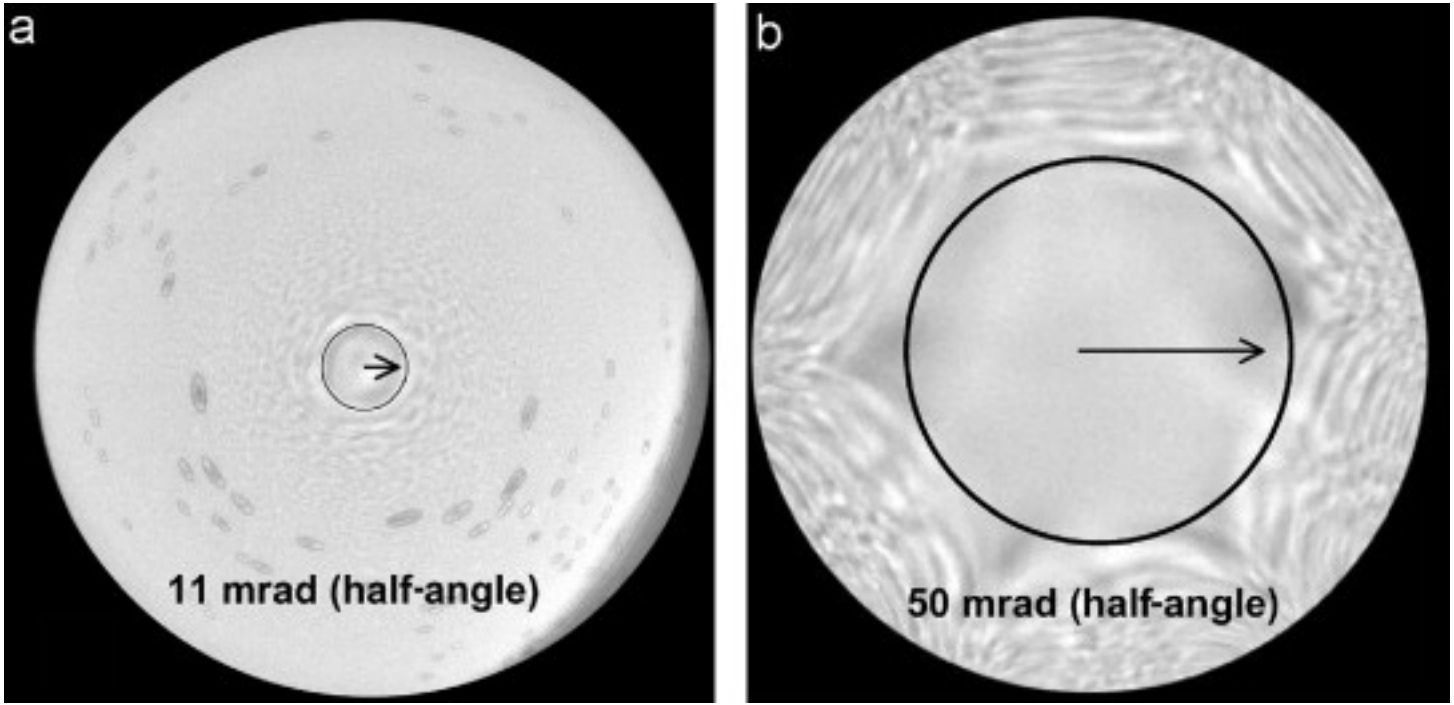

Cs corrected

Shadow image | Resolution

STEM resolution is detemined by the size of the probe and stability of the instrument

$$\alpha_{opt} = \left(\frac{4\lambda}{C_s}\right)^{\frac{1}{4}}$$

At optimum defocus and with the correct aperture size, the probe FWHM is given by:

$$d_{opt} = 0.61\ \frac{\lambda}{\alpha_{opt}} = 0.43\ \lambda^{\frac{3}{4}}\ C_s{}^{\frac{1}{4}}$$

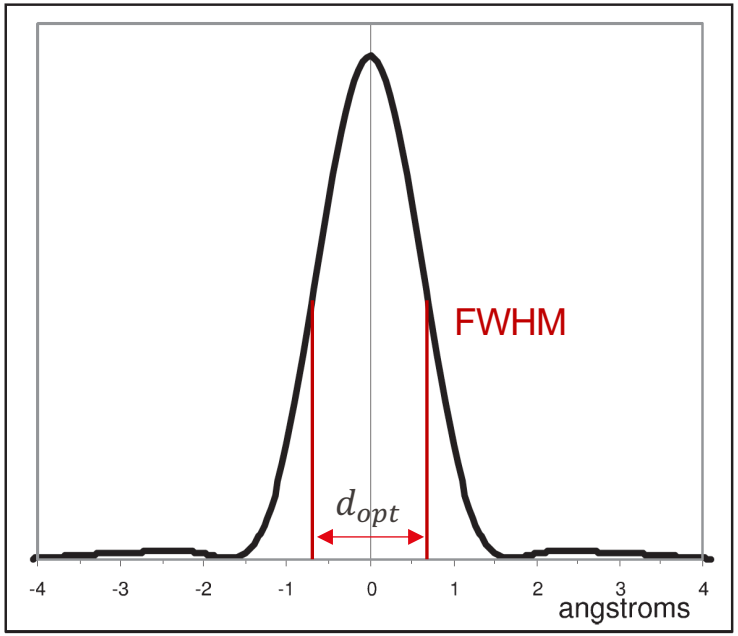

The intensity of a diffraction-limited STEM probe for the illumination conditions:
Cs 1mm, and defocus 35.5 nm, @200kV.

Spectrum imaging

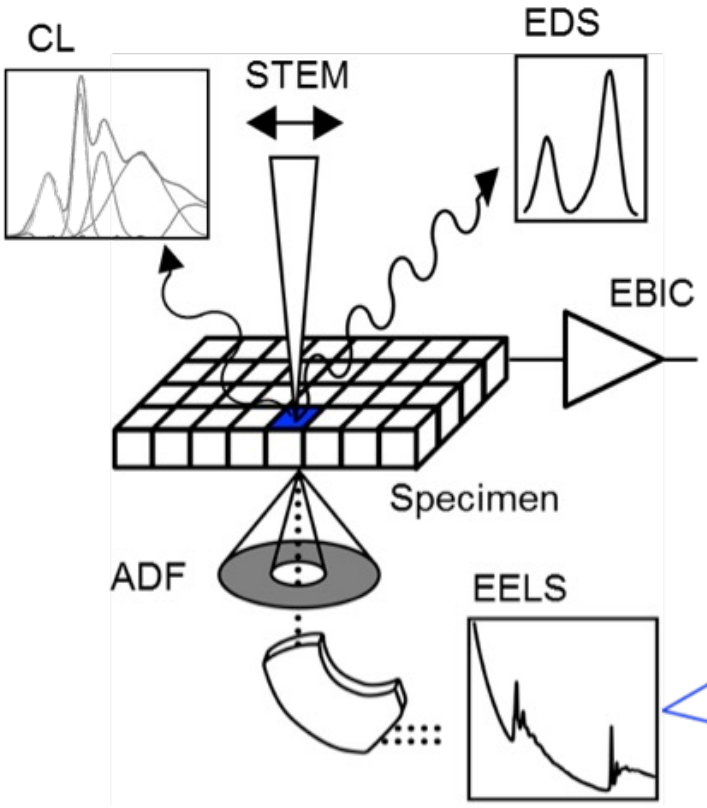

Record spectrum as function of probe position (x, y)

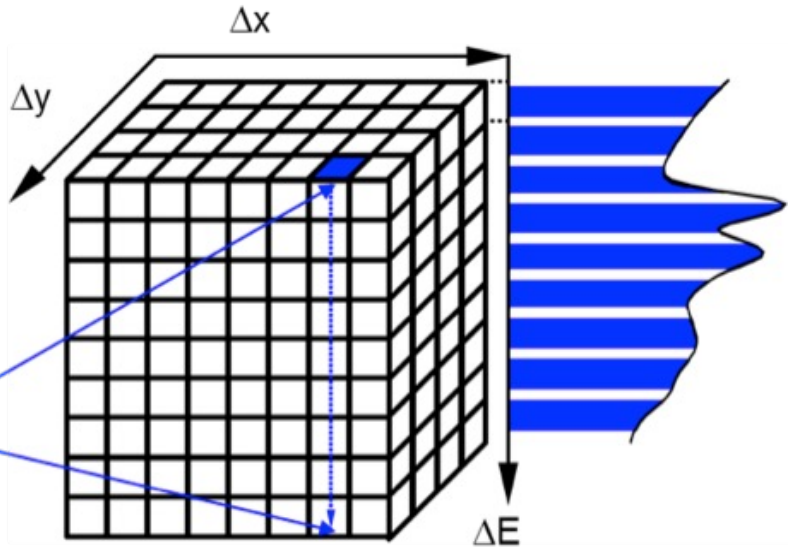

Image for Gatan.com

Energy-dispersive X-ray (EDX) STEM mapping

With fast mapping STEM-EDX has become a regular feedback tool for materials synthesis.

Sample characterized in a couple of minutes.

Example : Assembly of Fe_3O_4 and Cu particles

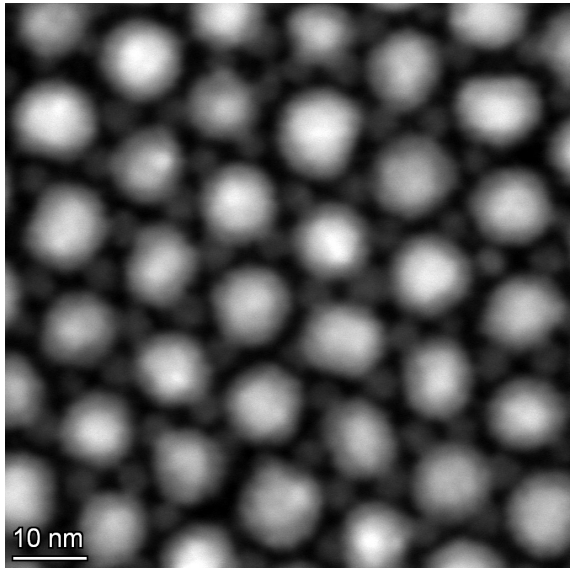

HAADF image

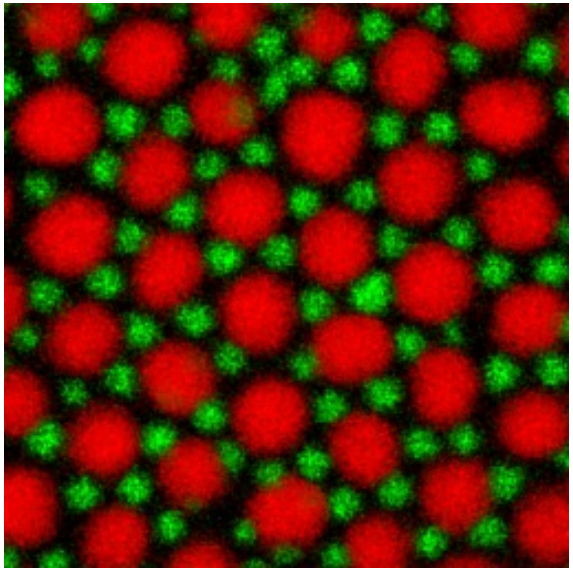

Map of Cu and Fe

In collaboration with Chethana Gadiyar LNCE, EPFL

J. Am. Chem. Soc. 2020, 142, 37, 15931–15940

Energy-dispersive X-ray (EDX) STEM mapping

With fast mapping STEM-EDX has become a regular feedback tool for materials synthesis.

Sample characterized in a couple of minutes.

Example : Ni-Rh catalytic nanoparticles in carbon shell

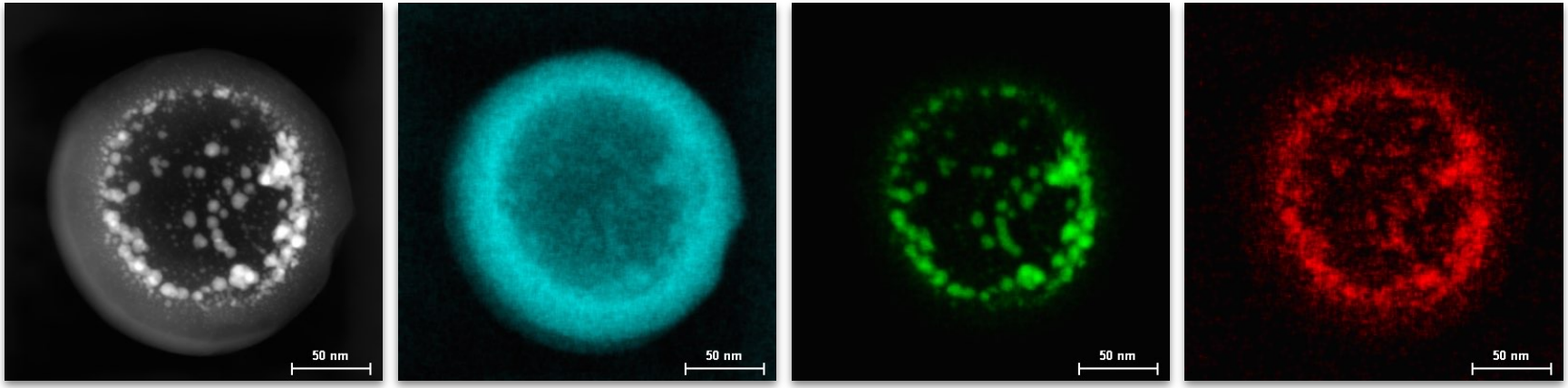

HAADF image

EDX maps of C, Rh and Ni

In collaboration with Chethana Gadiyar LNCE, EPFL

J. Am. Chem. Soc. 2020, 142, 37, 15931–15940

Energy-dispersive X-ray (EDX) STEM mapping

With aberration-corrected STEM, atomic resolution EDX became possible

Example: $(Ba_xSr_{1-x})TiO_3$

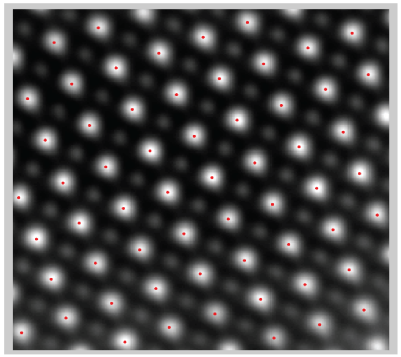

HAADF image

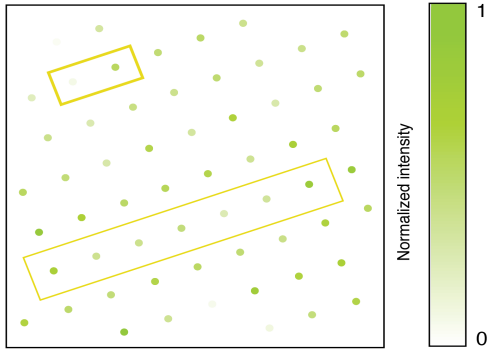

Intesnsity map

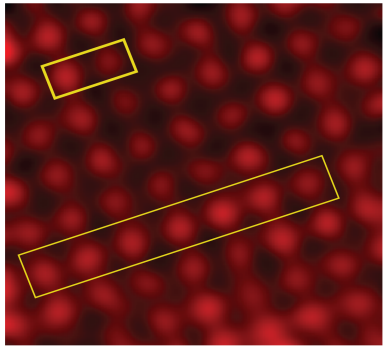

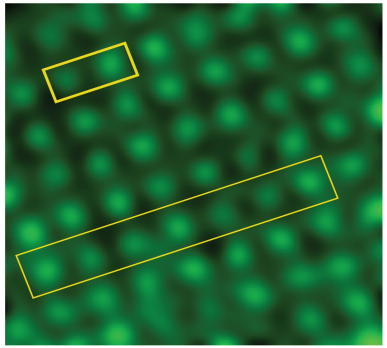

EDX maps of Sr and Ba

In collaboration with Prof. Dragan Damjanovic, EPFL
Bencan and Oveisi *et al*. Nature Communications 2021.

Electron energy-loss spectroscopy (EELS)

The S/TEM specific microanalysis technique!

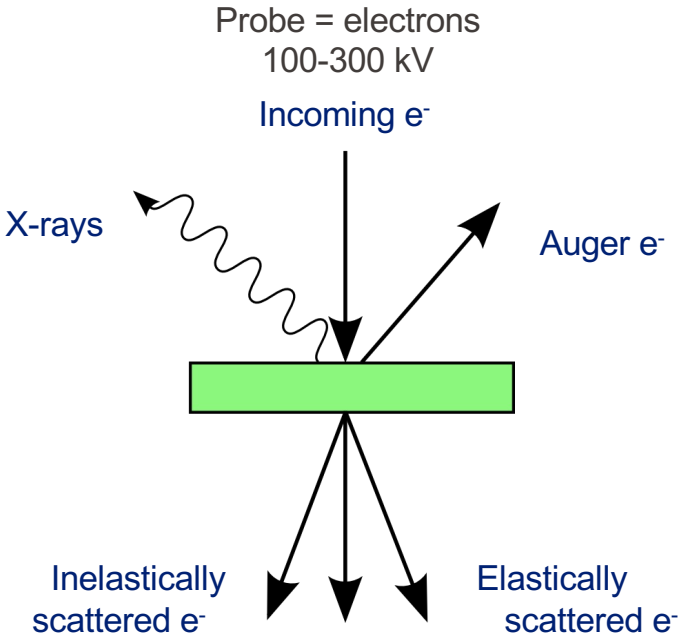

More details in Duncan Alexander's EELS lecture this afternoon

Principle of energy-loss spectrometry

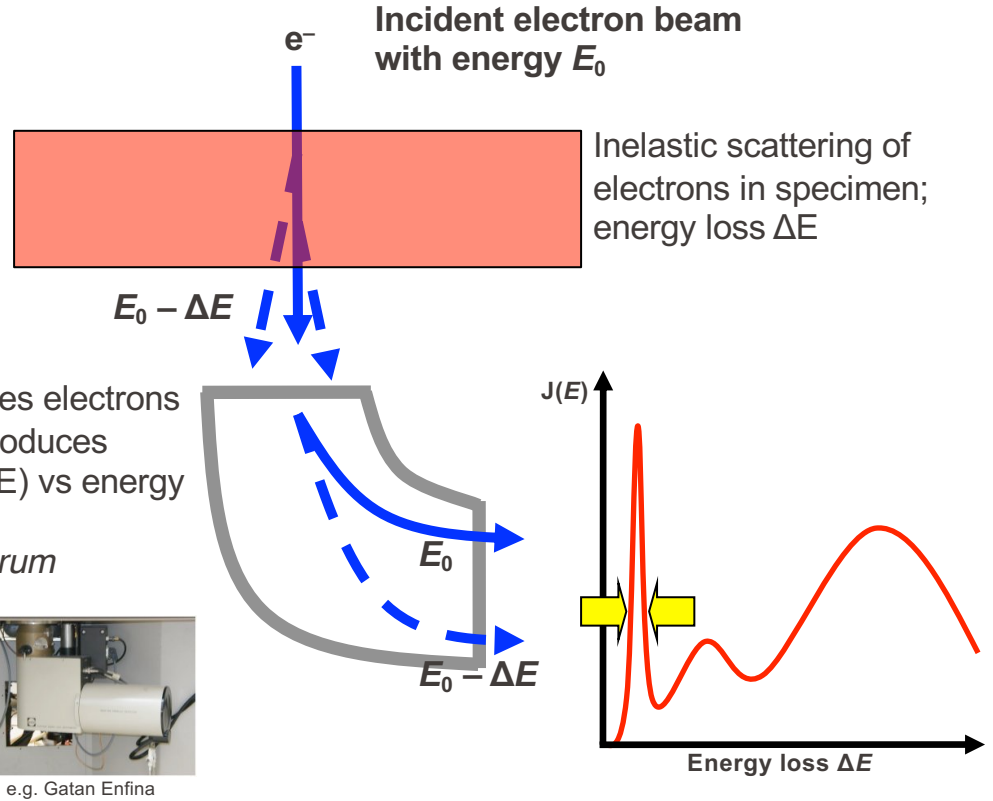

Atomic resolution core-loss STEM-EELS

Example: Atomic resolution spectroscopic imaging of a $La_{0.7}Sr_{0.3}MnO_3$ / $SrTiO_3$ multilayer, showing the different chemical sublattices in a 64 × 64 pixel spectrum image extracted from 650 eV–wide electron energy-loss spectra recorded at each pixel.

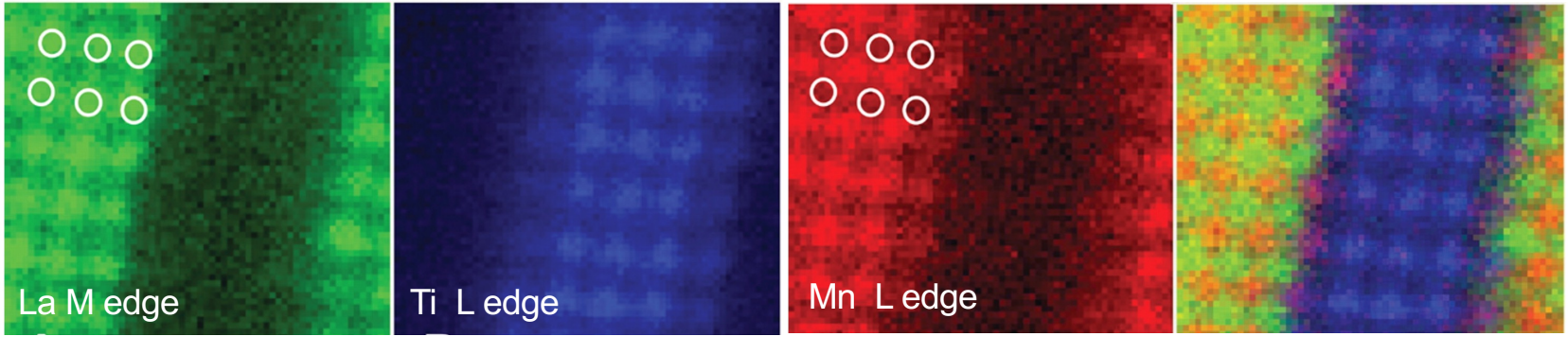

D.A Muller *et al.*, Science 2008.

Sample quality and imaging concerns

Emad Oveisi

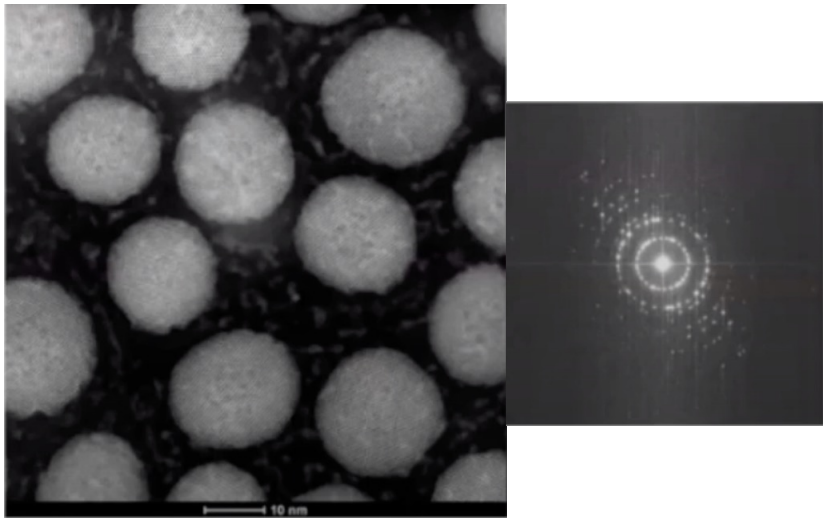

Without sample drift

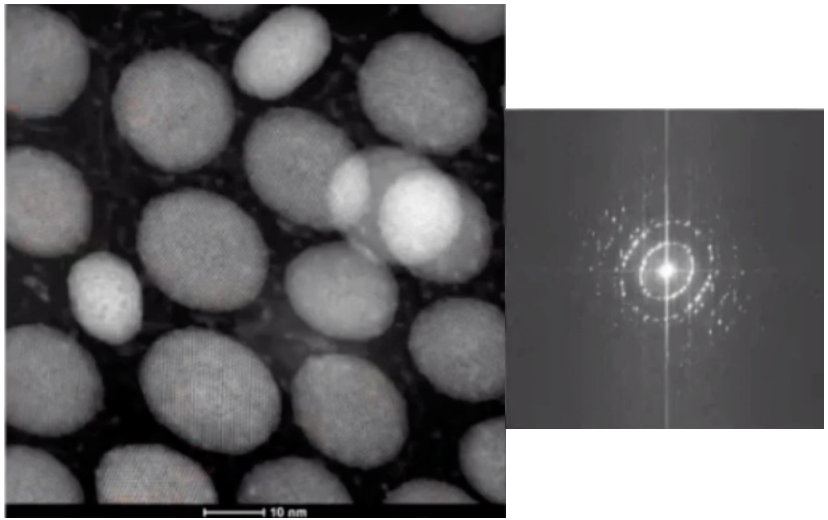

With sample drift

Sample quality and imaging concerns

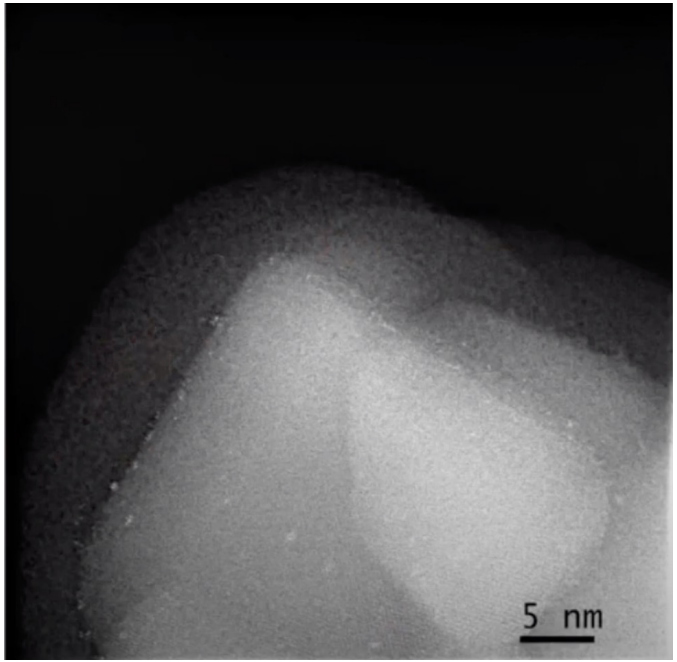

Beam induced contamination

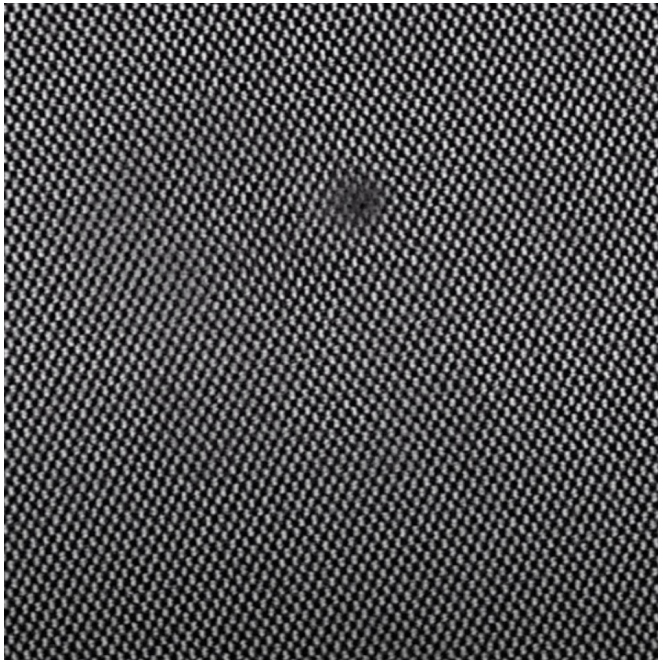

Beam induced damage (hole)

Emad Oveisi

Sample quality and imaging concerns

Represenatative of sample

Thin

Stabe under vaccum and probe current

Free of contamination

Uniform thickness for qunatative measurements

Conductive

Summary

- Aberration-correction and improved instrument stability give sub-Å resolution in STEM.
- With lower beam voltages, lighter elements can be analyzed without beam damage.
- Faster, more sensitive spectrometers give unprecedented access to composition, chemistry and physics of materials.
- Computer interfaces and software allow acquisition and processing of large datasets.
- STEM is now not one technique that can be easily summarized, but is split into many specialisms.
- Many other possible uses (e.g. imaging of magnetic domains, optical plasmon mapping, *in situ* studies) exist. The new equipment at CIME cover the majority of these possibilities, creating a state-of-the-art facility at EPFL.
- With the latest instrumentation, the sample and specimen preparation are often the limiting factor!

Some useful literature

- ✓ Scanning Transmission Electron Microscopy by S.J. Pennycook and P.D. Nellist (eds) (Springer)
- ✓ Aberration-corrected imaging in transmission electron microscopy: an introduction by R. Erni
- ✓ Transmission Electron Microscopy by D.B. Williams and C.B. Carter (Springer)
- ✓ Large Angle Convergent Beam Electron Diffraction by J.-P. Morniroli
- ✓ Transmission Electron Microscopy and Diffractometry of Materials, Fultz and Howe
- ✓ Science of Microscopy by C.W. Hawkes and J.C.H. Spence (eds) (Springer)